

INFORMATION TO USERS

This manuscript has been reproduced from the microfilm master. UMI films the text directly from the original or copy submitted. Thus, some thesis and dissertation copies are in typewriter face, while others may be from any type of computer printer.

The quality of this reproduction is dependent upon the quality of the copy submitted. Broken or indistinct print, colored or poor quality illustrations and photographs, print bleedthrough, substandard margins, and improper alignment can adversely affect reproduction.

In the unlikely event that the author did not send UMI a complete manuscript and there are missing pages, these will be noted. Also, if unauthorized copyright material had to be removed, a note will indicate the deletion.

Oversize materials (e.g., maps, drawings, charts) are reproduced by sectioning the original, beginning at the upper left-hand corner and continuing from left to right in equal sections with small overlaps. Each original is also photographed in one exposure and is included in reduced form at the back of the book.

Photographs included in the original manuscript have been reproduced xerographically in this copy. Higher quality 6" x 9" black and white photographic prints are available for any photographs or illustrations appearing in this copy for an additional charge. Contact UMI directly to order.

UMI

**A Bell & Howell Information Company
300 North Zeeb Road, Ann Arbor MI 48106-1346 USA
313/761-4700 800/521-0600**

University of Alberta

Heliphos and Its Transition Metal Complexes: Design and Synthesis

by

Yiming Yao ©

**A thesis submitted to the Faculty of Graduate Studies and Research in partial fulfillment of
the requirements for the degree of Master of Science**

Department of Chemistry

Edmonton, Alberta

Spring, 1997



National Library
of Canada

Acquisitions and
Bibliographic Services

395 Wellington Street
Ottawa ON K1A 0N4
Canada

Bibliothèque nationale
du Canada

Acquisitions et
services bibliographiques

395, rue Wellington
Ottawa ON K1A 0N4
Canada

Your file Votre référence

Our file Notre référence

The author has granted a non-exclusive licence allowing the National Library of Canada to reproduce, loan, distribute or sell copies of his/her thesis by any means and in any form or format, making this thesis available to interested persons.

The author retains ownership of the copyright in his/her thesis. Neither the thesis nor substantial extracts from it may be printed or otherwise reproduced with the author's permission.

L'auteur a accordé une licence non exclusive permettant à la Bibliothèque nationale du Canada de reproduire, prêter, distribuer ou vendre des copies de sa thèse de quelque manière et sous quelque forme que ce soit pour mettre des exemplaires de cette thèse à la disposition des personnes intéressées.

L'auteur conserve la propriété du droit d'auteur qui protège sa thèse. Ni la thèse ni des extraits substantiels de celle-ci ne doivent être imprimés ou autrement reproduits sans son autorisation.

0-612-21228-9

University of Alberta

Release Form

Name of Author: Yiming Yao
Title of Thesis: Heliphos and Its Transition Metal Complexes:
Design and Synthesis
Degree: Master of Science
Year this Degree Granted: 1997

Permission is hereby granted to the University of Alberta to reproduce single copies of this thesis and to lend or sell such copies for private, scholarly, or scientific research purposes only.

The author reserves all other publication and other rights in association with the copyright in the thesis, and except as herein before provided, neither the thesis nor any substantial portion thereof may be printed or otherwise reproduced in any material form whatever without the author's prior written permission.


Yiming Yao

204, 9904-90 Avenue
Edmonton, Alberta
Canada, T6E 2T3

April 2, 1997

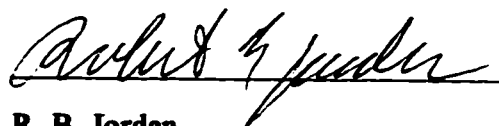
University of Alberta

Faculty of Graduate Study and Research

The undersigned certify that they have read, and recommend to the Faculty of Graduate Studies and Research for acceptance, a thesis entitled **Heliphos and Its Transition Metal Complexes: Design and Synthesis** submitted by Yiming Yao in partial fulfillment of the requirement for the degree of Master of Science.



S. H. Bergens



R. B. Jordan



G. Kwon

March 27, 1997

Abstract

(R)- and *(S)*- 1, 2-bis(diphenylphosphino)-2-(diphenylphosphinomethyl)-1-phenylpropane (*(R)*- and *(S)*-heliphos) were synthesized via an acid catalyzed diastereoselective Michael addition of diphenylphosphine to di-(1*R*, 2*R*, 3*R*)-(-)-menthyl benzylmalonate. The rhodium complex [(heliphos)Rh(NBD)](ClO₄) was prepared by reaction of heliphos with [Rh(NBD)₂](ClO₄). The crystal structure of [(*(R)*-heliphos)Rh(NBD)](ClO₄) was determined by X-ray diffraction. The *(R)*-heliphos adopted the predicted Λ -conformation in the solid state, and NMR experiments indicated that it strongly favors this conformation in solution as well. The sense of helicity was controlled by the absolute conformation of the stereogenic carbon atom in the ligand.

Attempts to use [(heliphos)Rh(NBD)](ClO₄) as an enantioselective catalyst were hampered by phosphine arm dissociation. The reaction of heliphos with ruthenium resulted mainly in the formation of compounds in which heliphos acted as a bidentate ligand.

Acknowledgments

First, I would like to thank my research advisor Dr. Bergens for his guidance and encouragement.

Christopher J. A. Daley is gratefully acknowledged for his allowing me to include his work in this dissertation.

Next, I would like to thank all of the members of the Bergens research group, they were the source of stimulating and fruitful discussions on many topics, including chemistry.

Finally, I would like to thank my parents for their unconditional support. A special thanks is given to my wife Fenqiu for her patience and understanding, and for helping me keep things in perspective.

Table of Contents

Chapter	
1. Chiral Tripodal Ligands, their Metal Complexes and Catalysis	1
1.1 Introduction	1
1.2 Chiral Tripodal Ligands with Nitrogen and Oxygen Atoms as Donors	4
1.3 Chiral Tripodal Tris(phosphine)	11
1.4 Catalysis	18
1.5 Conclusion	20
2. Design and Synthesis: Heliphos and Its Rhodium Complex	21
2.1 Design of Heliphos	21
2.2 Synthesis of Heliphos	23
2.3 Synthesis and Characterization of [(heliphos)Rh(NBD)](ClO ₄)	30
2.4 Solid and Solution Conformational Study of [((R)-heliphos)Rh(NBD)](ClO ₄)	35
2.5 Conclusion	37
3. Catalysis	43
3.1 Catalytic Reactions	43
3.2 Conclusion	45
4. Ruthenium Compounds of Heliphos	46
4.1 Synthesis	46
4.2 Conclusion	49
Experimental Section	51
References	66

List of Figures

Figure 1.1	Tripodal ligands with chirality in the backbone.	4
Figure 1.2	The molecular structure of the cationic portion of [Co(NCS)(<i>S</i>-tan)](ClO₄). Hydrogen atoms have been omitted for clarity.	5
Figure 1.3	The molecular structure of the cationic portion of Zn(α-MeBQPA)Cl](ClO₄). Some hydrogen atoms have been included in calculated positions.	6
Figure 1.4	The molecular structure of {(<i>R, R, R</i>)-N[CH₂CH(^tBu)O]₃}VO.	8
Figure 1.5	Tripodal ligands with chirality in nitrogen ancillary groups.	9
Figure 1.6	The molecular structure of [HB(Methpz)₃ZnCl]. Hydrogen atoms have been omitted for clarity.	11
Figure 1.7	Chiral tripodal phosphine ligands.	12
Figure 1.8	The molecular structure of the cationic portion of [(tris(((2<i>S</i>, 5<i>S</i>)-2, 5-dimethylphospholano)methyl)methane)Rh(COD)](SbF₆). Hydrogen atoms have been omitted for clarity.	14
Figure 1.9	The molecular structure of the cationic portion of [((<i>R, R, R</i>)-Siliphos)Rh(NBD)](OTf). Hydrogen atoms have been omitted for clarity.	15
Figure 1.10	The molecular structure of [CH₃C(CH₂P(Et)Ph)₃]Mo(CO)₃.	16
Figure 1.11	Tripodal phosphines containing phosphites or hetero atoms.	18
Figure 2.1	(Top) The molecular structure of the cationic portion of [((<i>R</i>)-heliphos)Rh(NBD)](ClO₄). Hydrogen atoms have been omitted for clarity; (Bottom) View looking down crystallographic <i>pseudo</i>-C₃ axis. NBD has been omitted for clarity.	31
Figure 2.2	³¹P{¹H} NMR spectrum of [(heliphos)Rh(NBD)](ClO₄).	32

Figure 2.3 ^1H (Bottom) and $^1\text{H}\{^3\text{P}\}$ (Top) NMR spectra of framework protons region of $[(\text{heliphos})\text{Rh}(\text{NBD})](\text{ClO}_4)$.

List of Abbreviations and Symbols

a	axial
Å	Angström (s); 10⁻¹⁰ m
atm	atmosphere (s)
BINAP	2, 2'-bis(diphenylphosphino)-1, 1'-binaphthyl
c	concentration
ca.	<i>circa</i> (approximately)
calcd	calculated
CD	circular dichroism
Camphpz	(4<i>S</i>, 7<i>R</i>)-7, 8, 8, trimethyl-4, 5, 6, 7-tetrahydro-4, 7-methano-2-indazoly
COD	1, 5-cyclooctadiene
COSY	correlated spectroscopy
deg	degree (s)
e	equatorial
ee	enantiomeric excess
Et	ethyl
heliphos	1, 2-bis(diphenylphosphino)-2-(diphenylphosphinomethyl)-1-phenylpropane
HPLC	high performance liquid chromatography
iPr	isopropyl
Me	methyl
α-MeBQPA	α-bis(2-quinolymethyl)-2-pyridyl-1-ethylamine
Mementhpz	7-(<i>R</i>)-isopyroyl-4-(<i>R</i>)-methyl-4, 5, 6, 7-tetrahydroindazolyl
Menth	(1<i>R</i>, 2<i>S</i>, 5<i>R</i>)-(-)-menthyl
Menthpz	7-(<i>R</i>)-<i>tert</i>-butyl-4-(<i>R</i>)-methyl-4, 5, 6, 7-tetrahydroindazolyl

Menthpz	7-(<i>R</i>)-<i>tert</i>-butyl-4-(<i>R</i>)-methyl-4, 5, 6, 7-tetrahydroindazolyl
α-MeTPA	α-methyl tris(pyridylmethyl)-amine
Ms	methanesulfonyl
MS	mass spectrometry
NBD	Norbormadiene
NMR	nuclear magnetic resonance
NOE	Nuclear Overhauser Effect
Ph	phenyl
ppm	parts per million
r. t.	room temperature
Siliphos	MeSi[CH₂P(^tBu)Ph]₃
<i>S</i>-tan	2, 4, 8-trimethyl-5-(3-methyl-3-azabutyl)-2, 5, 8-triaza-4(<i>S</i>)-nonane
^tBu	<i>tert</i>-Butyl
Tf	triflate
THF	tetrahydrofuran
triphos	1, 1, 1-tris(diphenylphosphinomethyl)ethane
Ts	<i>p</i>-toluenesulfonyl
TMEDA	N, N, N', N'-Tetramethylethylenediamine

Chapter 1

Chiral Tripodal Ligands, their Metal Complexes, and Catalysis

1.1 Introduction

Biological systems that are made up of chiral components often recognize enantiomers as different substances (as a result of diastereomeric relationships). For example, the *R*-isomer of thalidomide is a sedative drug, but the *S*-isomer causes profound birth defects in babies born to mothers using the drug.¹ The thalidomide tragedy would have been avoided if the pharmaceutical company marketed the optically pure drug instead of the racemate. Racemic drugs contain 50% of an isomer that usually has no therapeutic value but has the potential to cause deleterious side effects. Several methods, such as chiral chromatography, are available to separate enantiomers, but asymmetric synthesis is still the most important and practical way to obtain optically pure compounds.²

Conventional methods of asymmetric synthesis, including resolution and chiral pool synthesis, rely on the use of stoichiometric quantities of enantiomerically pure starting materials or reagents. Resolution is a process whereby a racemic product mixture is converted into a separable mixture of diastereomers, then separated by physical methods, such as distillation, crystallization, or chromatography. Chiral pool synthesis is the preparation of optically pure compounds from natural chiral sources. The main method used today for industrial production of enantiomerically pure drugs is resolution.³

The advantage of enantioselective catalysis is that it operates via chiral multiplication in which one molecule of optically pure catalyst can produce thousands of equivalents of chiral product. Multiplication of chirality is a characteristic feature of both biocatalysts and metal-based catalysts. Biocatalysts have been very successful in asymmetric synthesis especially in polypeptides, vitamins, and complicated carbohydrates.⁴

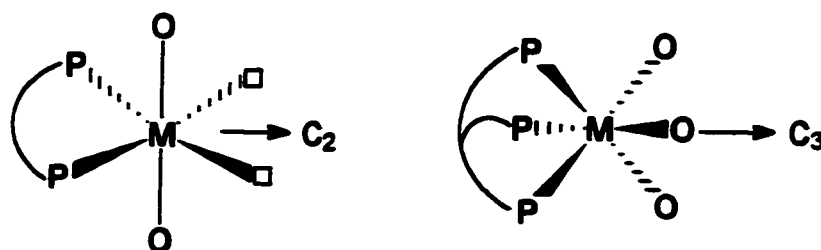
Chiral metal catalysts have many advantages over biocatalysts including that separation of products is relatively easy, that it is convenient to modify catalysts by changing ligands, and that metal complexes can catalyze reactions such as hydroboration that do not occur in nature.

Over the past two decades, asymmetric catalysis using chiral metal complexes has evolved into a dynamic, rapidly growing area of research. As a result, a large number of reactions have been reported.⁵ Several catalytic asymmetric reactions, including the "Monsanto process" (asymmetric hydrogenation),⁶ the "Takasago Process" (asymmetric isomerization),⁷ the "Sumitomo Process" (asymmetric cyclopropanation),⁸ and the "Arco Process" (asymmetric epoxidation)⁹ were commercialized in the 1980s. Despite these impressive achievements, the number of efficient, truly enantioselective catalysts is still limited. Thus, the major efforts of future research will continue to focus on improvement of existing catalysts and on the search for new catalysts.

Progress in the development of catalysts is made more often by serendipitous discovery than by systematic planning. However, some guidelines have been developed for the design of new ligands and catalysts. These are (a) use of conformationally rigid chiral ligands, (b) use of ligands possessing C_2 -symmetry, and (c) use of bidentate ligands and substrates. A common feature of these guidelines is the restriction of conformational variety available to the metal-ligand system. The great success of C_2 -symmetric bidentate ligands in asymmetric catalysis is attributed to the reduction of possible competing diastereomeric transition states.¹⁰ For example, in a square planar complex bearing a C_2 -symmetric bidentate ligand, the two remaining coordination sites are equivalent. The possible diastereomers for a complex containing C_2 -symmetric bidentate ligand will be less than a complex containing monodentate ligands or non-symmetric ligands.

For these reasons, Burk recently suggested that highly dissymmetric ligands, such as those possessing three-fold rotation axes, would lead to high enantioselectivity in catalytic reactions involving octahedral intermediates.¹¹ This hypothesis was based on the

following model study. Scheme 1.1 shows a C_2 -symmetric bidentate phosphine and a C_3 -symmetric tripodal phosphine coordinated to octahedral metal centres. There is only one



○ and □ represent vacant coordination sites.

Scheme 1.1

type of chiral site available for a substrate to coordinate to a catalyst containing the C_3 -symmetric ligand. In contrast, two types of chiral sites - axial and equatorial are available on the metal catalyst containing the C_2 -symmetric bis(phosphine). During the catalytic reaction, the number of possible diastereomers for the complex containing a C_3 -symmetric ligand will be less than that for the complex containing a C_2 -symmetric ligand.

As will be reviewed below, the number of chiral tripodal ligands reported in the literature is limited. Few catalytic reactions have been performed, and there remain many reactions that the current catalyst systems do not effect. The general objectives of this research are first, to design and synthesize a new chiral tripodal phosphine ligand that possesses a unique chirality, second, to investigate the solid state and solution conformation of the tripodal phosphine metal complex, and third, to investigate the enantioselectivity of the new tripodal phosphine metal complex in asymmetric catalysis.

1.2 Chiral Tripodal Ligands With Nitrogen and Oxygen Atoms as Donors

There are two general classes of chiral tripodal ligands using nitrogen and oxygen atoms as donor atoms. The first bear stereogenic centres in the carbon framework of the ligand as shown in figure 1.1. These ligands are tetradentate.

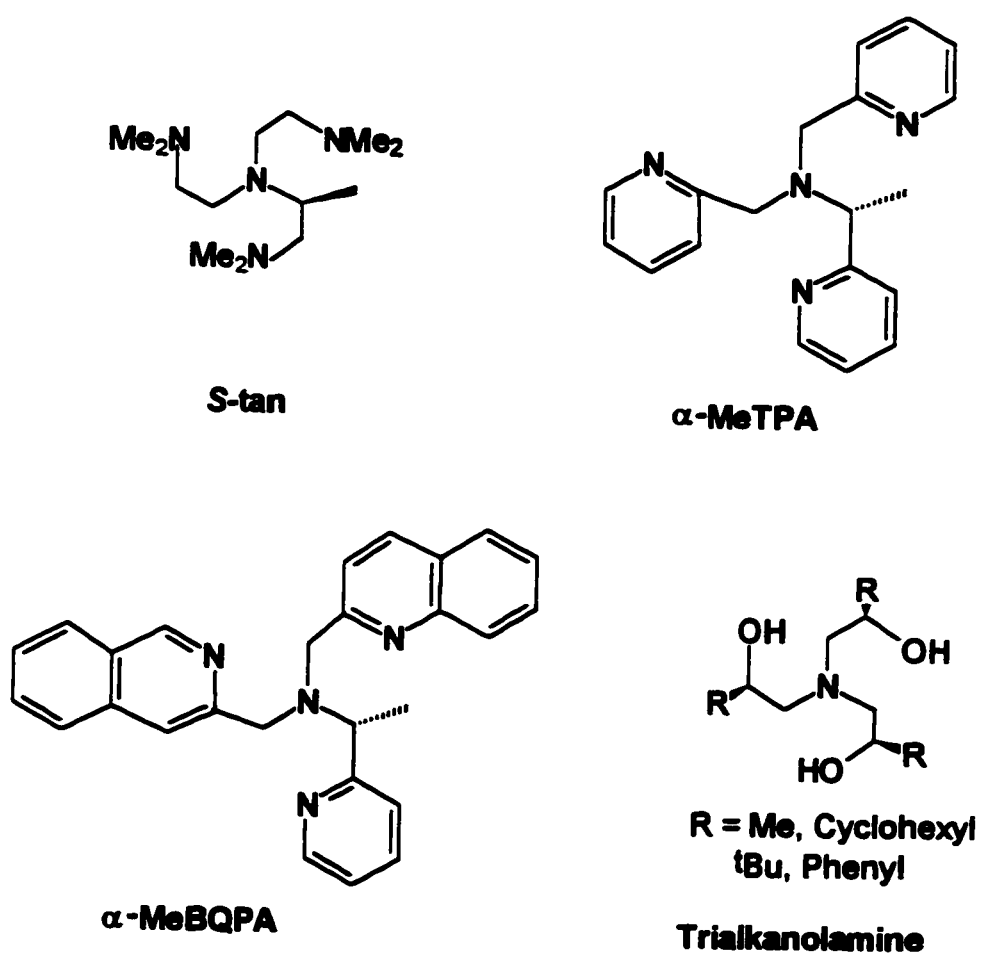


Figure 1.1 Tripodal ligands with stereogenic centres in the backbone.

Shunji Utsumo reported the first chiral tripodal ligand, $\text{Me}_2\text{NCH}_2\text{CH}(\text{Me})\text{N}[\text{CH}_2\text{CH}_2\text{N}(\text{Me})_2]_2$ (*S*-tan),¹² which was synthesized from L-

alanine. The crystal structure of the cobalt complex $[\text{Co}(\text{NCS})(S\text{-tan})](\text{ClO}_4)$ was determined and is presented in figure 1.2. The cobalt ion is surrounded by five nitrogen atoms in an approximate trigonal bipyramidal geometry. The cobalt lies $0.30(1) \text{ \AA}$ below the equatorial plane of the three nitrogen atoms of the *S-tan* molecule. The bond distances between cobalt and the three equatorial nitrogen atoms are similar ($2.13(1)$, $2.13(2)$, and $2.14(1) \text{ \AA}$). The notable feature of this structure is that all three five-membered chelate rings adopt the δ conformation. This is due to the preference of the methyl group at C(2) towards the equatorial position of the $\text{CoN}(1)\text{C}(2)\text{C}(3)\text{N}(2)$ five-member chelate ring. The methyl group would suffer steric repulsions if it was located in an axial position. Therefore the δ conformation in this complex is favoured when the absolute configuration at C(2) carbon is *S*.

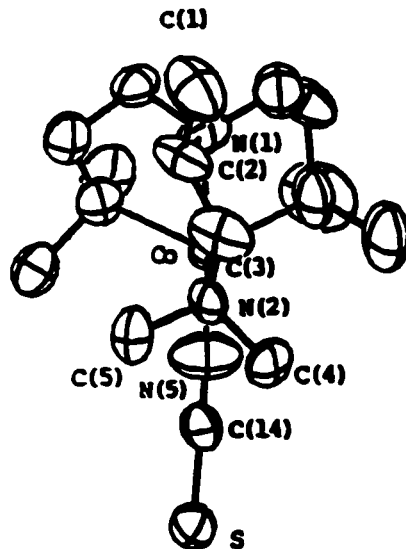


Figure 1.2 The molecular structure of the cationic portion of $[\text{Co}(\text{NCS})(S\text{-tan})](\text{ClO}_4)$. Hydrogen atoms have been omitted for clarity.

The solution conformation was studied by Circular Dichroism (CD) spectrometry. The CD spectrum predicted by the ligand-polarization model for the δ, δ, δ conformation (Δ -conformation) was comparable to the experimental CD spectrum.

Recently, ligands such as α -methyl tris(pyridylmethyl)-amine (α -MeTPA) and bis(2-quinolymethyl)-2-pyridyl-1-ethylamine (α -MeBQPA) were reported by Canary *et al.*¹³ The coordination chemistry of these ligands was investigated by preparing complexes with Zn(II) and Cu(II). The X-ray structure of $[\text{Zn}(\alpha\text{-MeBQPA})\text{Cl}](\text{ClO}_4)$ was determined and is shown in figure 1.3.

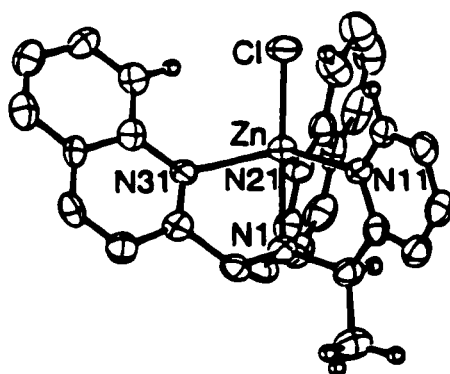


Figure 1.3 The molecular structure of the cationic portion of $[\text{Zn}(\alpha\text{-MeBQPA})\text{Cl}](\text{ClO}_4)$. Some hydrogen atoms have been included in calculated positions.

The geometry around the metal center is a twisted trigonal-bipyramidal with an average N(1)-Zn-N-C torsion angle of 16° [8.3(5), 13.9(5), 25.8(5)]. The pyridine rings occupy equatorial positions and display a propeller like pseudo- C_3 -symmetric arrangement (Δ -conformation). This helical conformation was controlled by the methyl

group at the stereogenic centre. The CD spectra of optically pure $[\text{Zn}(\alpha\text{-MeTPA})\text{Cl}](\text{ClO}_4)$ and $[\text{Cu}(\alpha\text{-MeTPA})\text{Cl}](\text{ClO}_4)$ show significantly enhanced signals compared with those of free ligands, indicating the presence of helical conformations in solution. These metal complexes acted as chiral solvating agents for sulfoxides and sulfides.

Nugent *et al.* have investigated a series of chelating homochiral trialkanolamines for several years.¹⁴ The syntheses of these ligands are simple. For example, (*S, S, S*)-trisisopropanolamine is conveniently prepared by reaction of commercial (*S*)-(+)-1-aminoisopropanol with two equivalents of (-)-propylene oxide in toluene. These ligands coordinate well to early transition metals and several such metal complexes were prepared, and demonstrated excellent enantioselectivity in asymmetric catalysis. For example, zirconium species bearing (*S,S,S*)-trisisopropanolamine catalyzed the enantioselective cleavage of meso epoxides with azidotrialkylsilanes. The reported ee of the product was up to 93%.

In order to understand the structural features imposed by these ligands on metal complexes, the solid state and solution structure of $\{(R, R, R)\text{-N}[\text{CH}_2\text{CH}(\text{tBu})\text{O}]_3\}\text{VO}$ was investigated. The X-ray structure of this complex is shown in figure 1.4. The molecule exhibits a *pseudo*- C_3 -symmetric structure and a distorted trigonal bipyramidal geometry. Three *tert*-butyl groups are distal to the vanadium centre while the three OCH hydrogen atoms are proximal to the vanadium atom. It was proposed that the *tert*-butyl groups have no direct impact on the chiral environment of the vanadium complex, and it is the hydrogens that influence the asymmetric environment. The three chelate rings adopt the λ conformation (Λ -conformation). This is expected because the *tert*-butyl groups must occupy equatorial positions in order to avoid the steric interactions with the other chelate rings.

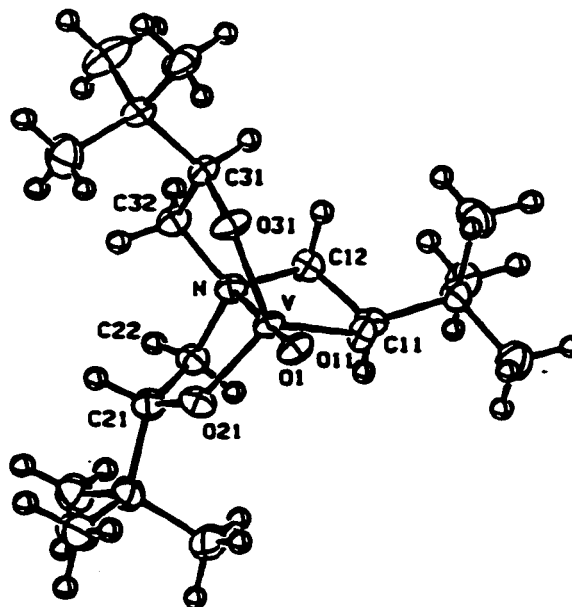


Figure 1.4 The molecular structure of $\{(R, R, R)\text{-N}[\text{CH}_2\text{CH}(\text{tBu})\text{O}]_3\}\text{VO}$.

NMR spectra of this complex recorded in CDCl_3 were consistent with the trigonal-bipyramidal C_3 -symmetry structure. The ^1H and ^{13}C NMR signals of all three arms were equivalent. The methylene protons ($-\text{CH}_2\text{N}-$) appeared as a doublet of doublets at 3.00 ppm and a *pseudo*-triplet at 2.82 ppm. The upfield methylene resonance had a large vicinal coupling (*ca.* 12 Hz), while the vicinal coupling for the downfield methylene resonance was smaller (*ca.* 4 Hz). The modest difference in diastereotopic shift (0.18 ppm), and the large difference in vicinal coupling constants (8 Hz) for the methylene protons indicated that the solution conformation was similar to the solid-state structure.

A interesting feature of this group of ligands is that they adopt helical conformations upon coordination to metal centres. Either Δ - or Λ - configurations are observed, depending on the substituents on the ligand's framework. In ethylenediamine or ethylenediphosphine complexes, it is known that the substituent has a steric preference for equatorial positions.^{10b} This tendency also is present in the tripodal ligand metal complexes.

The second type of chiral tripodal nitrogen-based ligands is shown in figure 1.5. These ligands possess stereogenic centres in the ancillary groups on nitrogen. Brunner reported the chiral tripodal ligand *R*-(+)-trisiminophos which was synthesized by Schiff base condensation of tris(2-formylphenyl) phosphane with (*R*)-(+)-1-phenylethylamine.¹⁵ There were no reports of characterized metal complexes of this C_3 -symmetric tetradentate ligand, but this was the first chiral tripodal ligand tested in asymmetric catalysis. A mixture of this ligand with the rhodium complex $[\text{Rh}(\text{COD})\text{Cl}]_2$ was used as catalyst for the enantioselective hydrogenation of (*Z*)- α -(acetylamino)cinnamic acid and for hydrosilylation of acetophenone. Less than 1% ee was reported.

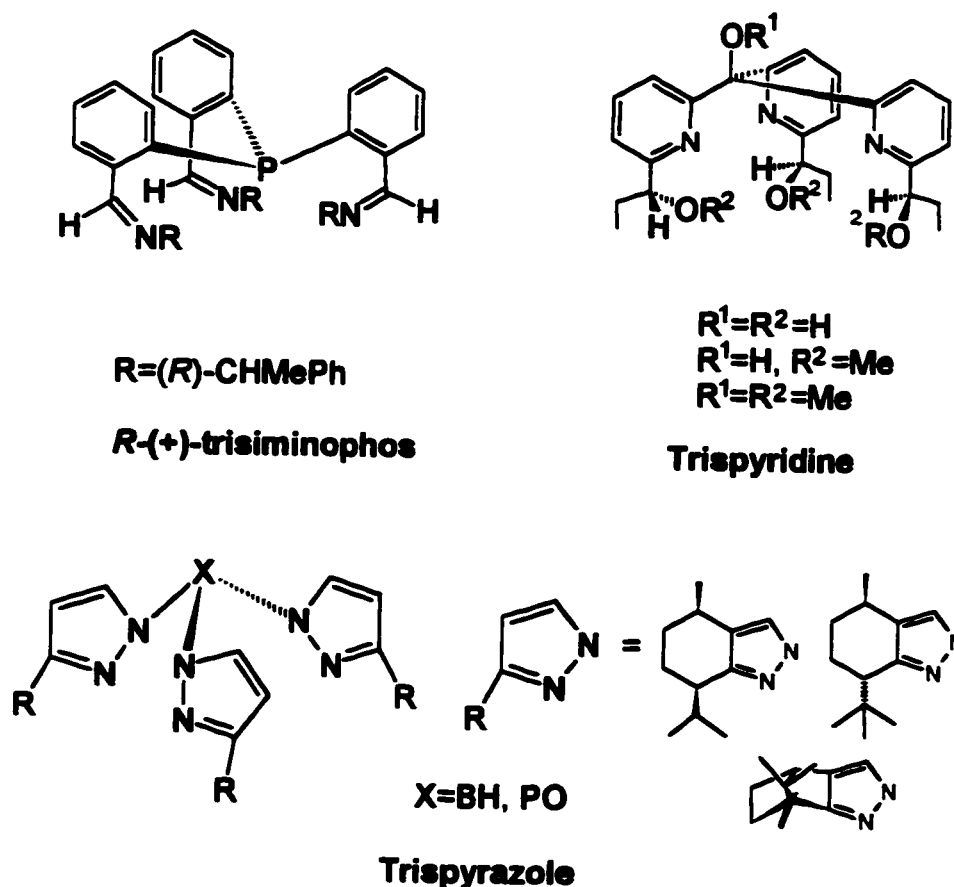


Figure 1.5 Tripodal ligands with stereogenic centres in nitrogen ancillary groups.

The C_3 -symmetric Trispyridine ligands were reported by Moberg in 1992.¹⁶ These ligands were prepared from tris(2-pyridyl) methanol. No characterized metal complexes of these C_3 -symmetric chiral ligand were reported. These ligands were not used in enantioselective catalysis.

Tris(pyrazolyl)hydroborate anions are well-established ligands in inorganic, organometallic, and bioinorganic chemistry.¹⁷ Their chiral analogs were reported by Tolman *et al.*¹⁸ A series of optically active C_3 -symmetric Trispyrazole ligands were designed and synthesized. The chiral tris(pyrazolyl)phosphine oxides were constructed by substitution of the chlorides in $OPCl_3$ by the appropriate chiral pyrazoles in the presence of triethylamine in refluxing benzene. The chiral tris(pyrazolyl)hydroborates were obtained by thermolysis of the chiral pyrazole in the presence of KBH_4 .

These ligands demonstrated their versatile metal binding properties by the isolation and characterization of complexes with $Zn(II)$, $Ni(II)$, $Cu(II)$, $Co(II)$, and $Tl(I)$. The C_3 -symmetric coordination mode was confirmed by NMR and X-ray diffraction. The structure parameters revealed that $[HB(Menthpz)_3ZnCl]$ and $[Tl(HB(Menthpz)_3)]$ (Menthpz = 7-(*R*)-isopyroyl-4-(*R*)-methyl-4,5,6,7-tetrahydroindazolyl) are slightly distorted from C_{3v} symmetry, while significant deviation from C_{3v} symmetry occurred in $[Tl(HB(Mementhpz)_3)]$ (Mementhpz = 7-(*S*)-*tert*-butyl-4-(*R*)-methyl-4,5,6,7-tetrahydroindazolyl). The crystal structure of $[HB(Menthpz)_3ZnCl]$ is shown in figure 1.6.

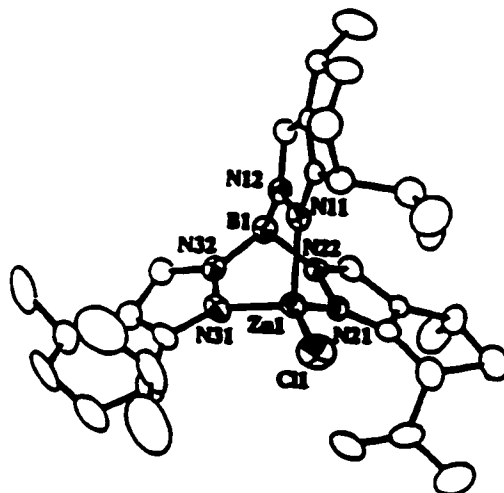


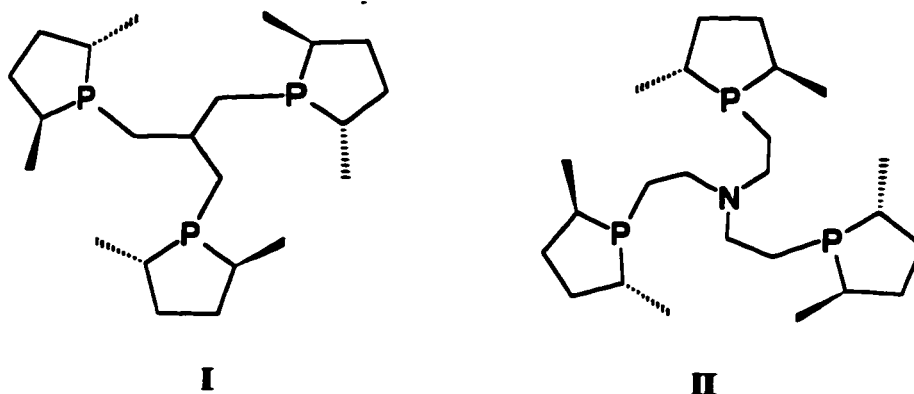
Figure 1.6 The molecular structure of $[\text{HB}(\text{Menthpz})_3\text{ZnCl}]$. Hydrogen atoms have been omitted for clarity.

The propeller-like disposition of alternating isopropyl (or isobutyl) groups around the ligand cavity in these complexes provides a unique and highly asymmetric environment which could greatly influence the enantioselectivity in asymmetric catalysis. Initial tests by the enantioselective cyclopropanation of styrene using $[\text{OP}(\text{Camphpz})_3\text{Cu}(\text{CH}_3\text{CN})](\text{BF}_4)$ as catalyst resulted in only moderate ee (< 60%).

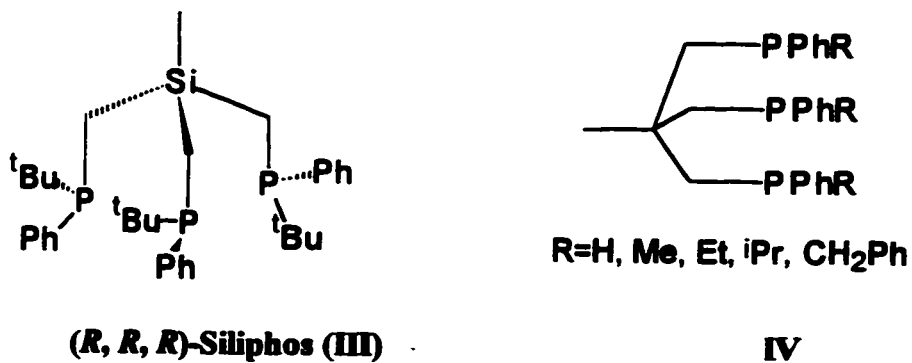
1.3 Chiral Tripodal Tris(phosphine)

Although achiral tripodal tris(phosphines) have been used in homogeneous catalysis for some time,¹⁹ their chiral analogs have only recently appeared in the literature. The first optically pure tripodal tris(phosphine) ligand I tris(((2*S*, 5*S*)-2, 5-dimethylphospholano)methyl)methane was reported by Burk in 1990.²⁰ The chiral tripodal tris(phosphine) ligands synthesized to date (figure 1.7) can be divided into three

Chiral Tripodal Phosphine Ligands with Stereogenic Centres in the Ancillary Groups.



Chiral Tripodal Phosphine Ligands with Stereogenic Centres at Phosphorus.



Chiral Tripodal Phosphine Ligands with three Different Phosphine Groups.

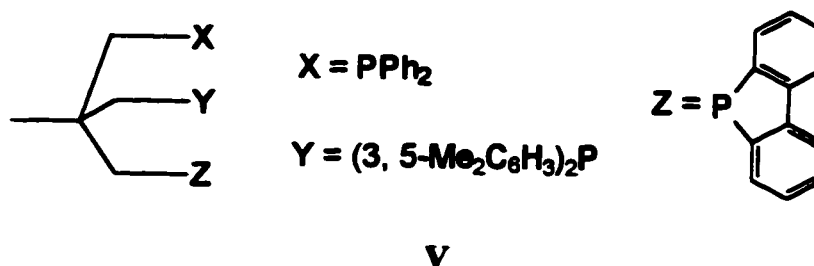
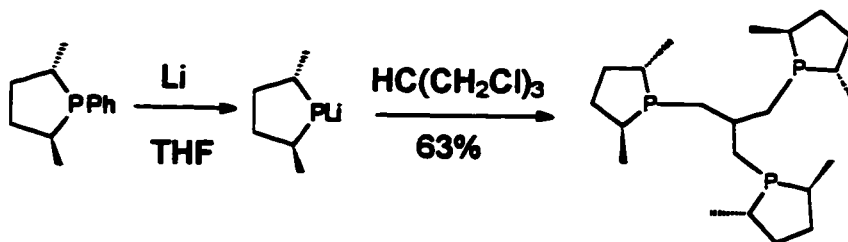


Figure 1.7 Chiral tripodal phosphine ligands

categories. These are chiral tripodal tris(phosphine) ligands with stereogenic centres in the ancillary groups attached to phosphorus, chiral tripodal tris(phosphine) ligands with stereogenic centres at the phosphorus atoms, and chiral tripodal tris(phosphine) ligands with three different phosphine groups.

The chiral tripodal ligand I was prepared by reaction of (2*S*, 5*S*)-2, 5-dimethyl-1-phenylphospholane with lithium, and reaction of the resulting phosphide with 1, 3-dichloro-2-(chloromethyl)propane as shown in scheme 1.2.



Scheme 1.2

The stereogenic centres of I are in the ancillary groups attached to phosphorus. The three-fold symmetry of this ligand was confirmed by ^{31}P NMR spectroscopy in C_6D_6 solution, which exhibited a singlet at -8.0 ppm. The corresponding rhodium(I) complex was prepared by reaction of I with $[\text{Rh}(\text{COD})_2](\text{SbF}_6)_3$. This complex was characterized by X-ray diffraction and the structure is presented in figure 1.8. As is apparent from the crystal structure, the phosphine-metal cage is twisted from C_{3v} symmetry. The C_3 -symmetric chiral tripodal phosphine imposes a highly asymmetric environment around the rhodium centre.

The ligand II was prepared from $\text{N}(\text{CH}_2\text{CH}_2\text{Cl})_3$. The rhodium (I) complex $[(\text{II})\text{Rh}(\text{CO})]\text{Cl}$ was also characterized by X-ray crystallography. The complex is trigonal bipyramidal in the solid-state, and it is C_3 -symmetric. This complex was not used in enantioselective catalysis.

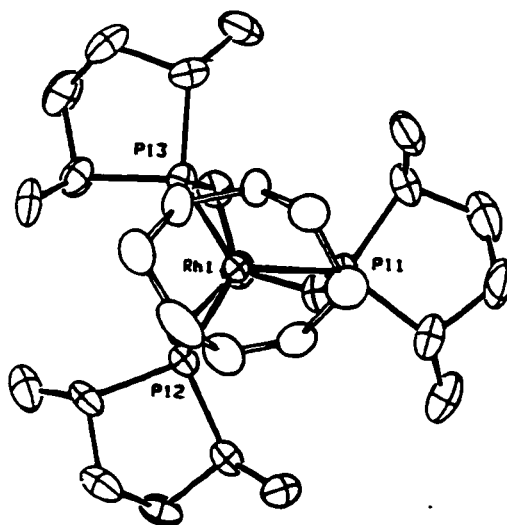
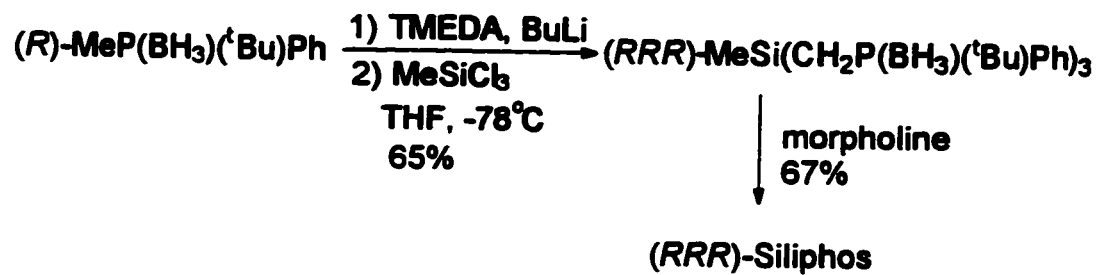


Figure 1.8 The molecular structure of the cationic portion of $[(I)Rh(COD)](SbF_6)$. Hydrogen atoms have been omitted for clarity.

Venanzi reported the homochiral tripodal phosphine (*R, R, R*)-Siliphos in which the phosphorus atoms are stereogenic.²¹ Deprotonation of (*R*)-(*tert*-butyl)(methyl)(phenyl)phosphine-borane followed by coupling with the electrophile $MeSiCl_3$ gave (*R, R, R*)-Siliphos in 45% yield.



Scheme 1.3

(R)-MeP(BH₃)(^tBu)Ph was obtained by separating the racemic phosphine-borane by chiral HPLC. Its rhodium complex was prepared by reaction of (*R, R, R*)-Siliphos with [Rh(NBD)₂](OTf) and the structure was confirmed by X-ray crystallography. The structure is presented in figure 1.9. The three P-Rh bond lengths are similar, 2.471 (9), 2.479 (8), and 2.489 (8) Å. The complex is *pseudo*-C₃-symmetric with the phenyl groups being parallel to the three-fold axis.

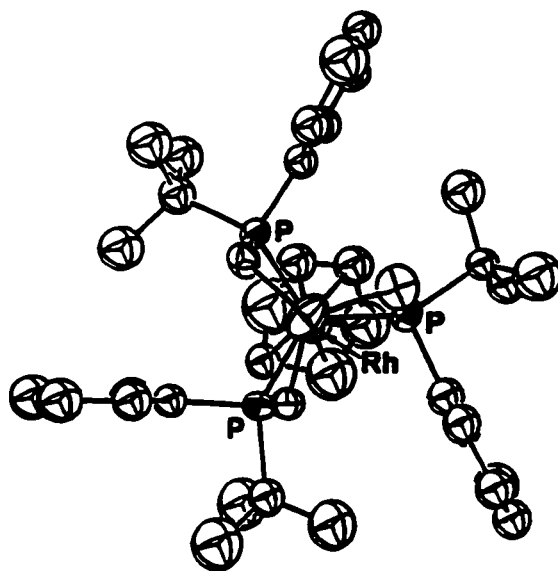
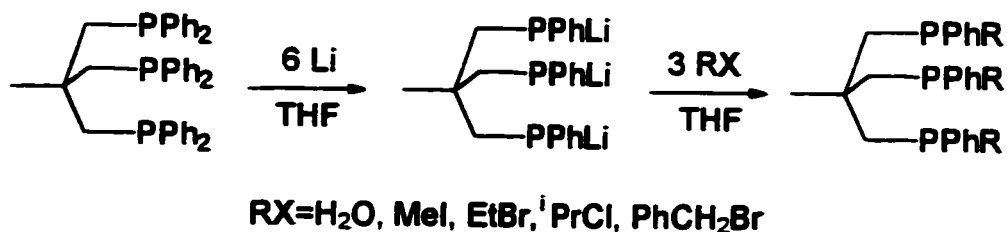


Figure 1.9 The molecular structure of the cationic portion of [((*R, R, R*)-Siliphos)Rh(NBD)](OTf). Hydrogen atoms have been omitted for clarity.

The chiral tripodal tris(phosphines) CH₃C[CH₂P(R)Ph]₃ (R = H, Me, ⁱPr, CH₂Ph) derived from triphos CH₃C(CH₂PPh₂)₃ have been prepared by Huttner *et al.*²² The entire transformation can be done in a one-pot procedure.



Scheme 1.4

The product was a mixture of diastereomers (*RRR/SSS:SSR/RRS*) in a ratio of 1:3. Only the *SSR/RRS* diastereomers formed if $\text{R} = \text{CH}_2\text{Ph}$. Molybdenum complexes of these ligands were prepared and the X-ray crystal structure of $[\text{CH}_3\text{C}(\text{CH}_2\text{P}(\text{Et})\text{Ph})_3]\text{Mo}(\text{CO})_3$ is presented in figure 1.10.

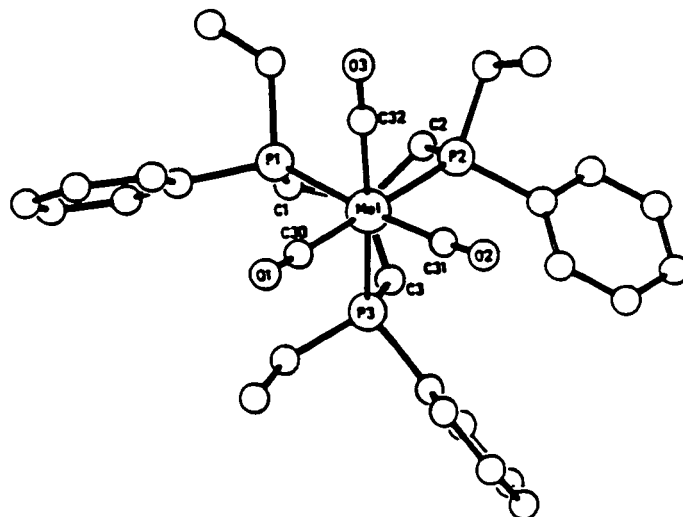
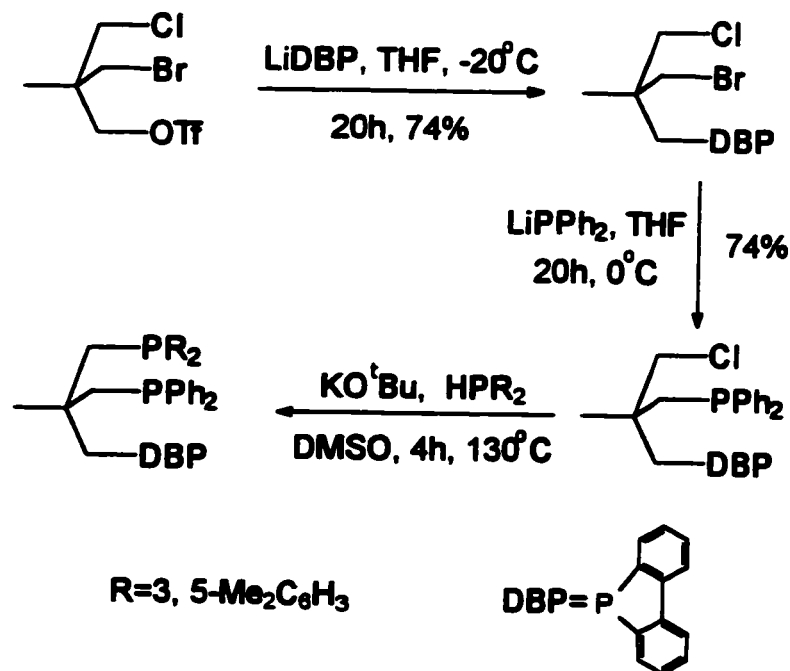


Figure 1.10 The molecular structure of $[\text{CH}_3\text{C}(\text{CH}_2\text{P}(\text{Et})\text{Ph})_3]\text{Mo}(\text{CO})_3$. Hydrogen atoms have been omitted for clarity.

As observed in those structures presented in figures 1.8 and 1.9, the tripodal phosphine twists into a helical conformation upon coordination. The resulting chiral

arrangement of pendent groups on phosphorus construct the asymmetric environment around the molybdenum centre. The optically pure form of these ligands is not available.

Huttner reported that successive phosphination of $\text{MeC}(\text{CH}_2\text{Cl})(\text{CH}_2\text{Br})(\text{CH}_2\text{OTf})$ with different phosphides gave the racemic chiral tripodal phosphine $\text{MeC}(\text{CH}_2\text{PR}'_2)(\text{CH}_2\text{PR}''_2)(\text{CH}_2\text{PR}'''_2)$ ²³ as shown in scheme 1.5. The synthesis of the starting tris(electrophile) is tedious and low yielding. The coordination behavior of these ligands was exemplified by the synthesis of $\text{MeC}(\text{CH}_2\text{PPh}_2)(\text{CH}_2\text{P}(3\text{-Tol})_2)(\text{CH}_2\text{P}(4\text{-Tol})_2)\text{Mo}(\text{CO})_3$. The optically pure ligand V shown in figure 1.7 was prepared by using enantiomerically pure starting compound $\text{MeC}(\text{CH}_2\text{Cl})(\text{CH}_2\text{Br})(\text{CH}_2\text{OTf})$.²⁴ No metal complex of the optically pure tripodal phosphine was reported.



Scheme 1.5

Several chiral tripodal phosphine ligands containing phosphite and hetero atoms (N, S) groups have also appeared in the literature recently, some even in enantiomerically pure form (shown in figure 1.11).²⁵ They will not be discussed in this thesis because these

ligands behave as bidentate ligands. There are no reports of any tripodal coordinated complexes of these ligands.

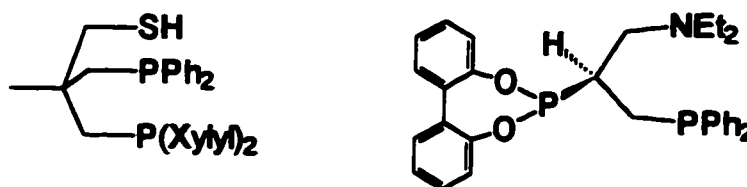
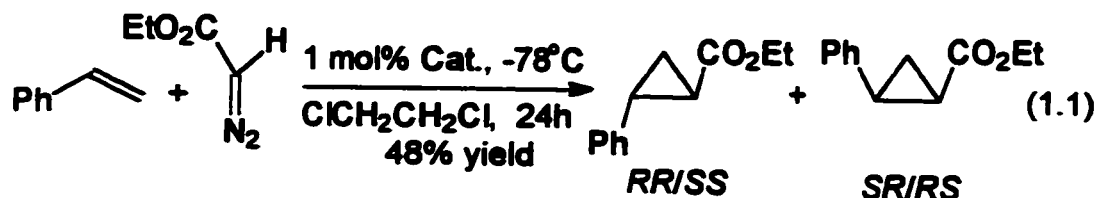


Figure 1.11 Tripodal phosphine containing phosphite or hetero atom groups.

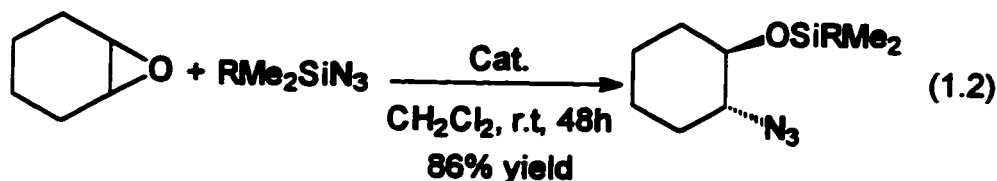
1.4 Catalysis

Several of the tripodal ligands discussed in the previous section have been used in enantioselective catalysis. Brunner was the first to use a chiral tripodal ligand in asymmetric catalysis.¹⁵ He used a mixture of (*R*)-(+)-trisiminophos and $[\text{Rh}(\text{COD})\text{Cl}]_2$ as a catalyst system for the enantioselective hydrosilylation of acetophenone. The hydrosilylation occurred with only low ee (< 1%).

Enantioselective catalysis using a chiral trispyrazole metal complex as catalyst also has been investigated.^{18a} Cyclopropanation of styrene using the diazo ester $\text{N}_2\text{CHCO}_2\text{C}_2\text{H}_5$ was catalyzed by $[\text{OP}(\text{Camphpz})_3\text{Cu}(\text{CH}_3\text{CN})](\text{BF}_4)$ (eq. 1.1). The ratio of *trans* to *cis* cyclopropane product was ~ 1:1.6. The ee of the *cis* product was 60%, and it was 40% for the *trans* product. The enantioselectivity exhibited only a moderate temperature dependence for both the *trans* and the *cis* products. By using the hindered aryldiazo ester (R = 2, 6-di-*tert*-butyl-4-methylphenyl), the *trans* to *cis* ratio improved to 23:1, but the ee decreased to 0% for the *cis* product, and to 10% for the *trans* product. Although only moderate enantioselectivity was observed, these results are a promising indication that chiral tripodal ligands are suitable for asymmetric synthesis.



Excellent enantioselectivity was obtained by Nugent *et al*^{14a} for the catalytic ring-opening of *meso*-epoxides by trialkylsilyl azides (eq. 1.2). The catalyst used was [(L-ZrOH)₂·^tBuOH]_n [L = (+)-(*S,S,S*)-trisisopropanolamine], synthesized from reaction between Zr(O^tBu)₄ and the C₃-symmetric tripodal ligand (+)-(*S,S,S*)-trisisopropanolamine, followed by partial hydrolysis. The catalytic reaction was carried out by combining the catalyst (8 mol%), trimethylsilyl trifluoroacetate (2 mol%), the trisalkylsilyl azide, and the epoxide. The trimethylsilyl trifluoroacetate was used to enhance the Lewis acidity of the catalyst and to improve the enantioselectivity. Using bulky azides, such as ⁱPrMe₂SiN₃, also improved the enantioselectivity. Enantiomeric excesses up to 93% were reported using cyclohexene oxide.



[(I)Rh(COD)](SbF₆) is the only chiral tripodal phosphine metal complex that has been used as a catalyst precursor in enantioselective catalysis.¹¹ Hydrogenation of methyl acetaminocinnamate and dimethyl itaconate gave 89% and 95% ee respectively. However longer reaction times (72 h) and higher temperatures (50 °C) were required for the hydrogenation of methyl acetaminocinnamate by the tripodal catalyst than those required by bis(phosphine) rhodium catalysts. A further increase in temperature (65°C) led to a dramatic decrease in enantioselectivity (40% ee). Similar results were observed for

hydrogenation of dimethyl itaconate. The requirement for high temperatures suggested that dissociation of one arm of the tripodal tris(phosphine) is necessary for the hydrogenation.

1.5 Conclusions

Although the number of chiral tripodal ligands is limited compared to that of chiral bidentate ligands, impressive enantioselection has been achieved using chiral tripodals in certain reactions. Solid-state and solution studies indicated that the asymmetric environment near the active sites on these metal catalysts are controlled by the conformations of the tripodal ligand.

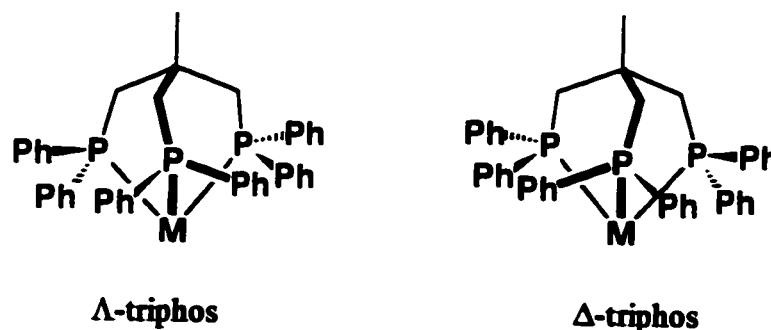
There are only four chiral tripodal phosphine ligands available in optically pure form. The stereogenic centers in these ligands are either at the phosphorus atoms, at the ancillary groups attached to the phosphorus atoms, or at the central carbon of the framework. There is another source of chirality that has not been explored for tripodal tris(phosphine) ligands, the helical conformations they adopt upon coordination to metal centres. Control over these helical conformations will control the configurations of the pendant groups on the phosphorus atoms. It is these pendant groups that make up the asymmetric environment around the active sites on the metal centre.

Chapter 2

Design and Synthesis: Heliphos and its Rhodium Complex

2.1 Design of Heliphos

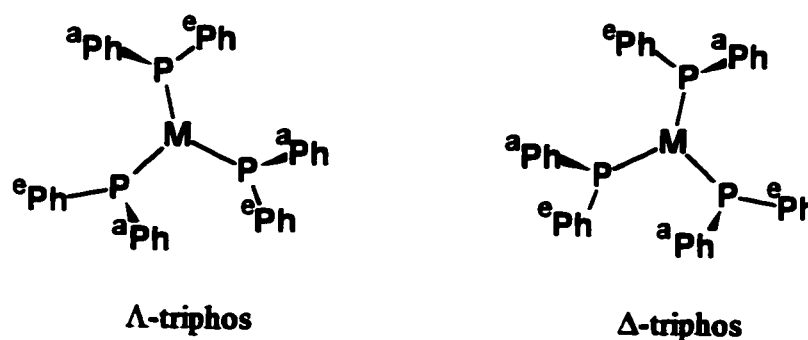
Published crystal structures of complexes containing tripodal phosphines (including those presented in figure 1.8 to 1.10) revealed that the tripodal phosphine metal cage is twisted into either left- or right-handed helices.²⁶ Shown below are the left (Λ)- and right (Δ)-handed helical conformers of coordinated 1, 1, 1-tris(diphenylphosphinomethyl)ethane (triphos).



Scheme 2.1

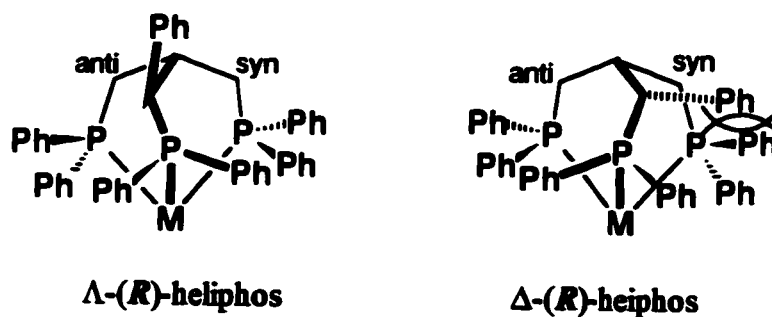
The Λ - and Δ -conformers are enantiomers that contain chiral arrays of pendant phenyl groups attached to phosphorus. As shown in scheme 2.2 from the perspective of the active sites on the metal centre, one phenyl group on each ligand arm projects towards the active sites (axial), while the other phenyl group resides roughly in the plane defined by the phosphorus atoms (equatorial). Interconversion between Λ - and Δ -triphos causes the equatorial and the axial phenyl groups to exchange orientations. A systematic conformational study of the tripodal phosphine metal complexes $[(\text{CH}_3(\text{CH}_2\text{Ph}_2)_3\text{CoL}_n$ ($n = 2, 3$)] using space group scatter graphs, principal component analysis, and partial least

squares has been reported recently.²⁷ The analysis showed that there are two classes of low energy conformations that differ by the handedness of the helicity.



Scheme 2.2

Molecular models show that replacement of a *pro-R* methylene proton in $\text{CH}(\text{CH}_2\text{PPh}_2)_3$ by a phenyl group imposes a severe steric repulsion between the added phenyl group and an equatorial phenyl group on the *syn*-arm of the Δ -conformer. This interaction is absent in the Λ -conformer. Conversely, replacement of a *pro-S* methylene proton imposes this interaction on the Λ -conformer, but it is absent from the Δ -conformer. The absolute configuration of the stereogenic centre in the framework can therefore be used to dictate which helical conformation is preferred by the coordinated ligand. These interactions are shown below for (*R*)-1,3-bis(diphenylphosphino)-2-(diphenylphosphinomethyl)-3-phenylpropane ((*R*)-heliphos).

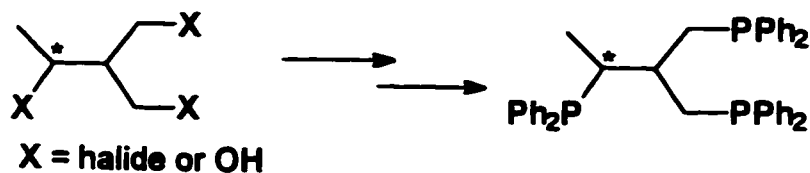


Scheme 2.3

Control over the absolute configuration of the stereogenic carbon in the ligand's framework should therefore dictate the absolute configuration of the asymmetric environment around the active sites on the metal centre.

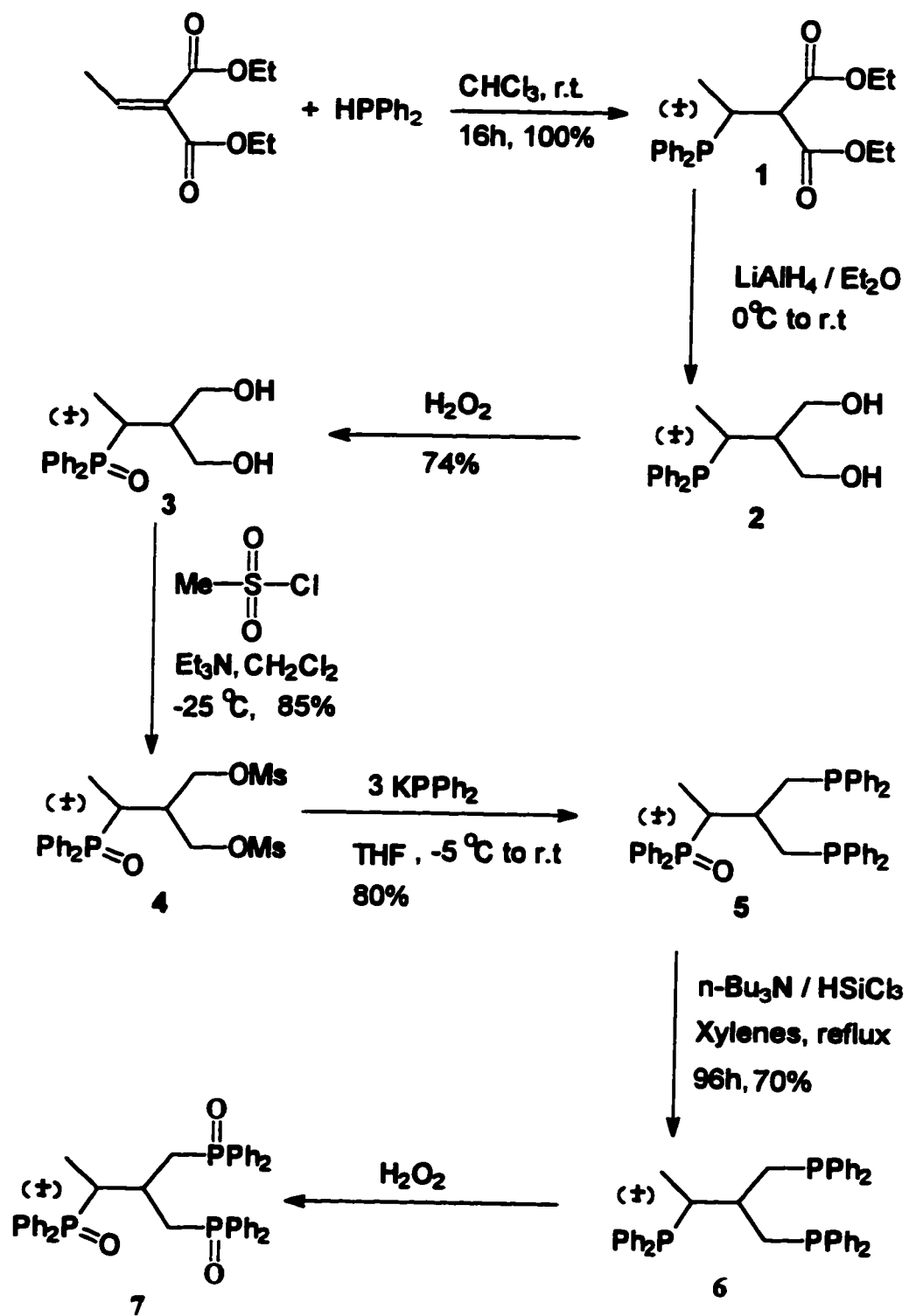
2.2 Synthesis of heliphos

There are many methods reported in the literature to synthesize optically pure phosphine ligands.²⁹ Most use either optically pure starting materials, or they use resolution of the racemic product phosphines. Both methods have been used to prepare chiral tripodal phosphines. One possible synthesis of heliphos would be the use of a tris(alcohol) or a tris(halide) such as 1, 3-dichloro-2-(chloromethyl)-1-methylpropane (scheme 2.4). This synthetic strategy was abandoned because these precursors are not readily available and they proved difficult to synthesize.



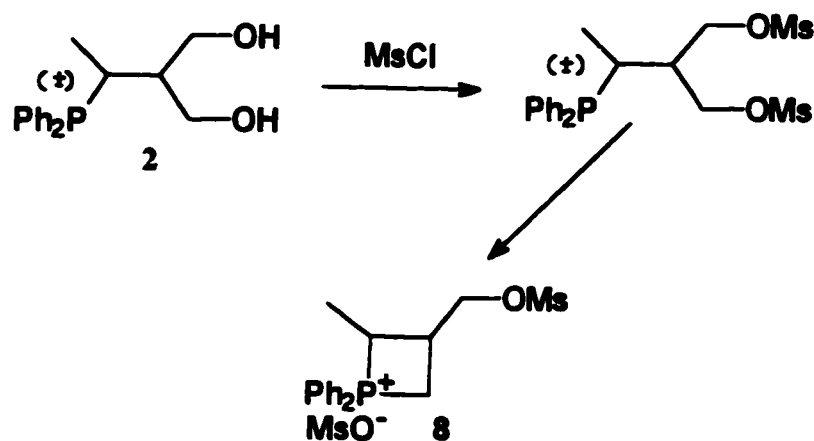
Scheme 2.4

An alternative route to the chiral tripodal phosphine was designed and proved successful. This procedure that was used to synthesize racemic 1, 3-bis(diphenylphosphino)-2-(diphenylphosphinomethyl)-1-methylpropane (**6**, a close analog of heliphos) is outlined in scheme 2.5. Commercially available diethyl ethylenemalonate was reacted with potassium diphenylphosphide and then treated with a saturated aqueous solution of ammonium chloride to quantitatively give the Michael product **1**. This Michael addition was accomplished more efficiently by stirring a mixture of HPPH_2 and diethyl



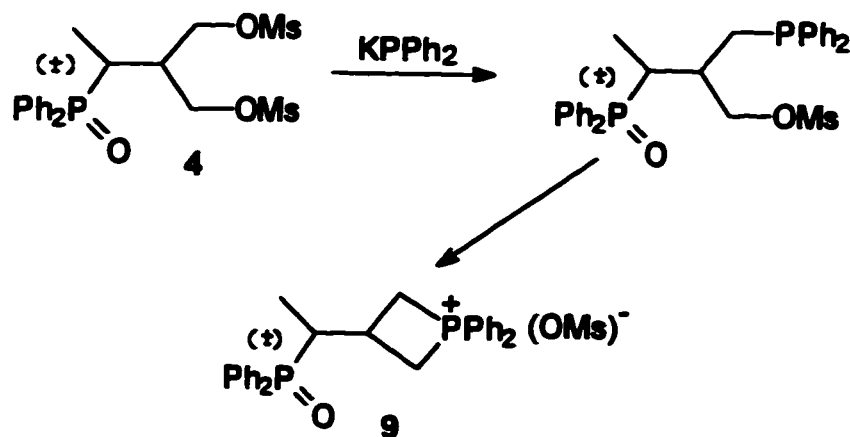
Scheme 2.5

ethylidenemalonate in CHCl_3 at room temperature. The Michael product **1** was then reduced to the corresponding phosphine-diol **2** by LiAlH_4 in ether. Mesylation of **2** by mesylchloride in the presence of triethylamine did not give the expected phosphine-dimesylate, rather an intramolecular displacement of a mesyl group by the phosphine occurred as shown in scheme 2.6. ^1H and ^{31}P NMR spectroscopy suggested that the phosphonium salt **8** formed. Attempts to make the phosphine bis(chloride) also failed for the same reasons. To avoid the intramolecular displacement reaction, the phosphine-diol **2** was oxidized to phosphine-oxide-diol **3** with a 10% aqueous solution of hydrogen peroxide (scheme 2.5).



Scheme 2.6

Mesylation of **3** gave the phosphine-oxide dimesylate **4** in high yield. The phosphine-oxide dimesylate **4** was reacted with potassium diphenylphosphide to give the tripodal phosphine monoxide **5**. This reaction was carried out by inverse addition of **4** to KPPH_2 . Addition KPPH_2 to **4** resulted in formation of **9** by intramolecular displacement of a mesyl group as shown in scheme 2.7.



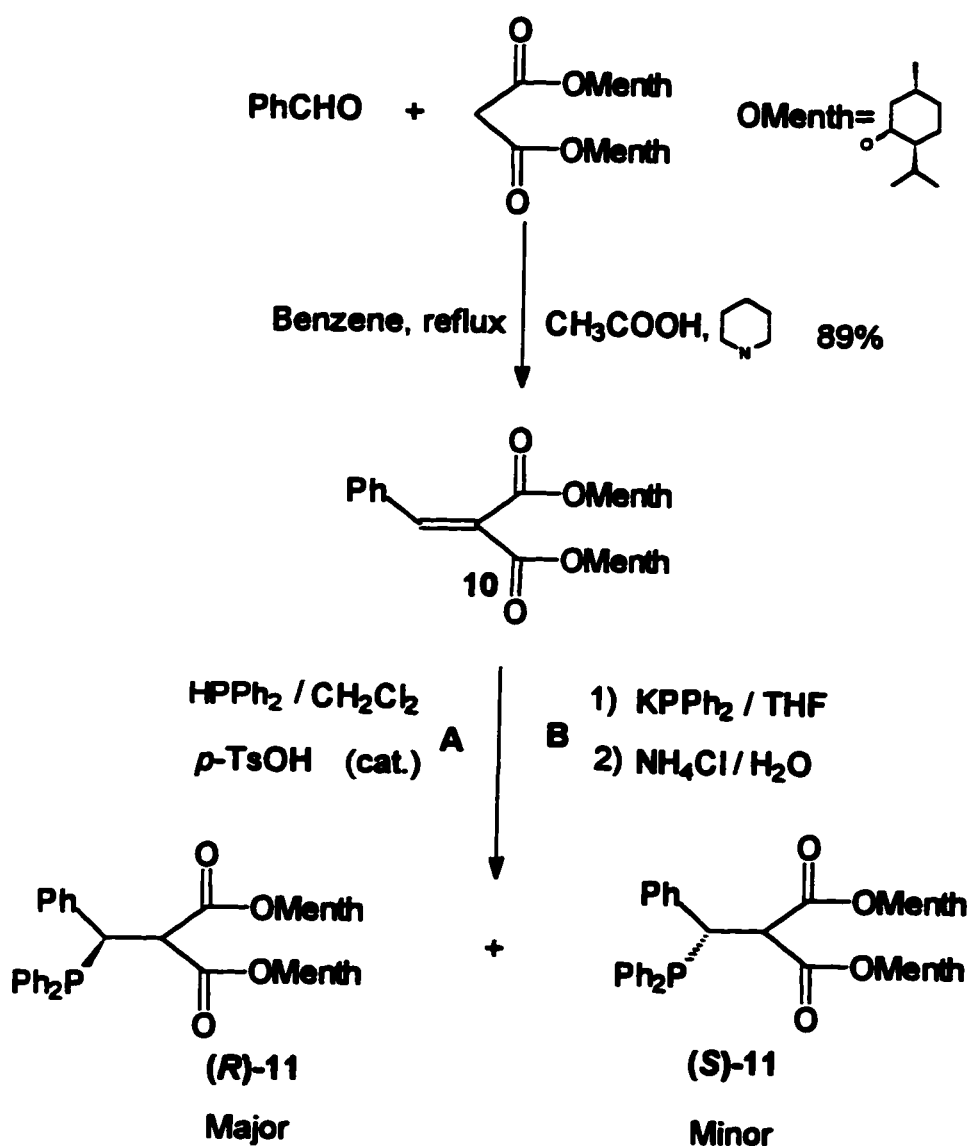
Scheme 2.7

Reduction of the monoxide **5** by trichlorosilane/tributylamine in refluxing xylene occurred in low yield because of evaporation of trichlorosilane. After four days, the reduction was only 75% complete.

Racemic **6** (containing 25% **5**) was oxidized to the tris(phosphine oxide) **7** with a 10% aqueous solution of hydrogen peroxide. The tris(phosphine oxide) **7** was purified by recrystallization from ether. Chiral organic acids are known resolving reagents for phosphine oxides.^{28b, 29} Three optically pure acids that have been used as resolving reagents, dibenzoyl-*l*-tartaric acid, *d*-10-camphorsulfonic acid and (1*R*, 3*S*)-(+)-camphoric acid, were used in an attempt to resolve racemic **7**. Two diastereomers were observed in ³¹P NMR spectra recorded of the **7** in the presence of the acids, but they could not be separated by fractional crystallization or by chromatography. The failure to resolve racemic **7** led to development of an alternative synthesis. The idea was to separate the enantiomers at the initial stage of the synthesis (scheme 2.8).

Optically pure Michael acceptors were prepared by condensation of dimethylmalonate with various aldehydes. The reaction between acetaldehyde and dimethylmalonate was hindered by self-condensation of acetaldehyde. Optically pure di-(1*R*, 2*S*, 5*R*)-(-)-menthyl benzylmalonate **10** was obtained by changing acetaldehyde to

benzaldehyde (scheme 2.8). Recrystallization from methanol afforded **10** in 89% yield. Michael addition of diphenylphosphine to **10** catalyzed by *p*-toluenesulfonic acid was diastereoselective generating diastereomers (*R*)-**11** and (*S*)-**11** in a ratio of 7 to 3. The two diastereomers were successfully separated by fractional recrystallization from mixed solvents (methanol/toluene) to give 80% yield of (*R*)-**11** and 64% yield of (*S*)-**11**. These



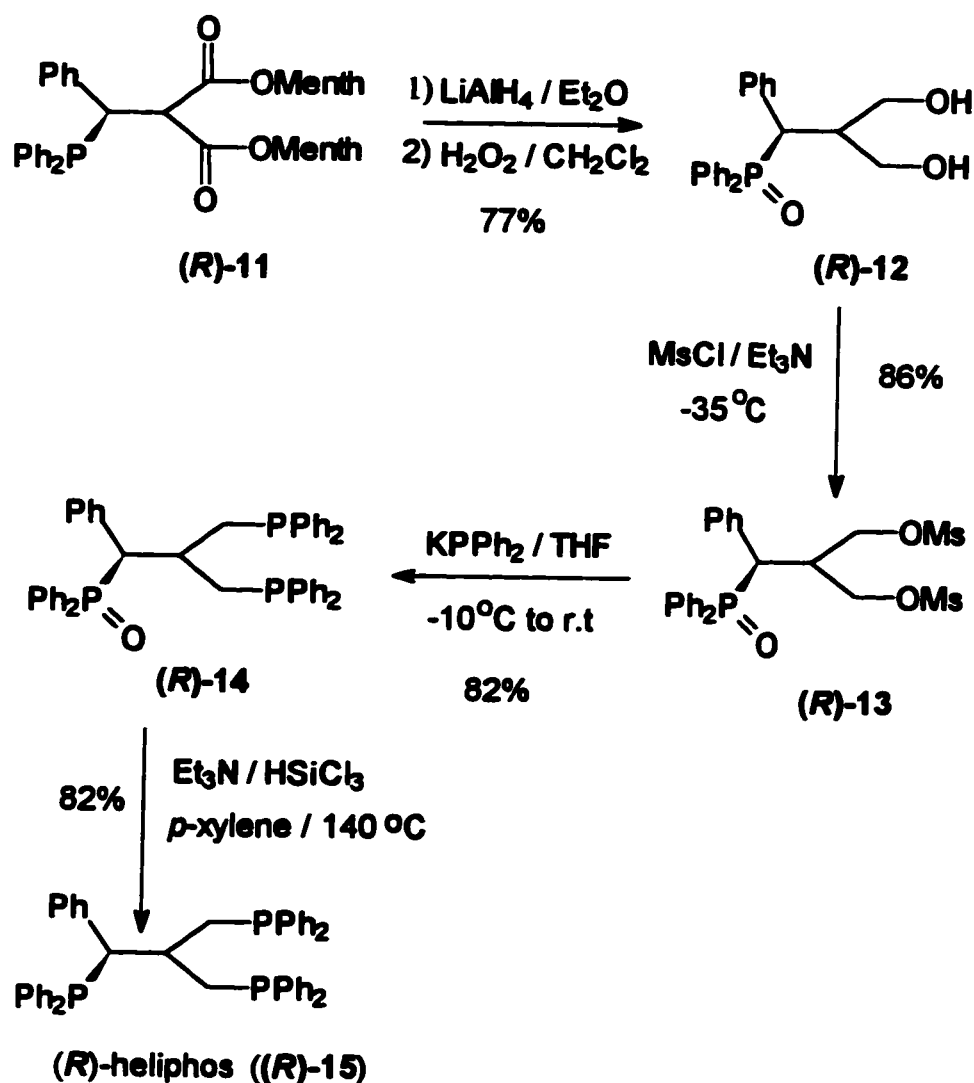
Scheme 2.8

yields could be improved by carefully repeating the isolations and recrystallizations.

Addition of potassium diphenylphosphide to 10 in THF and subsequent treatment with a saturated aqueous solution of ammonium chloride also led to (*R*)-11 and (*S*)-11, but with different diastereoselectivity (5.9:4.1).

The remaining steps are similar to the synthesis of 6 shown in scheme 2.9.

Optically pure (*R*)-11 and (*S*)-11 were reduced by LiAlH_4 in ether to give a mixture of the corresponding phosphine-diol and menthol. The phosphine-diol was separated from menthol by recrystallization from toluene. As before, the resulting phosphine was



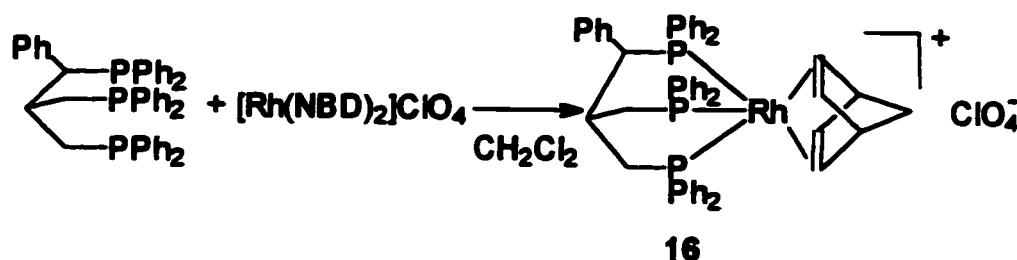
Scheme 2.9

oxidized by H_2O_2 , and the oxide (*R*)-12 was mesylated to produce the phosphine oxide dimesylate (*R*)-13. Displacement of the mesylate groups with potassium diphenylphosphide gave the optically pure phosphine oxide bis(phosphine) (*R*)-14. When the potassium diphenylphosphide was generated from KH and HPPh_2 , excess HPPh_2 over KH was required to avoid racemization via deprotonation of the slightly acidic proton at the chiral center in (*R*)-13 by KH. (*R*)-14 was reduced to the enantiomerically pure tripodal phosphine (*R*)-heliphos ((*R*)-15) by trichlorosilane/triethylamine in a high pressure reactor. Use of a sealed high pressure reactor prevented the evaporation of trichlorosilane. Crystallization from methanol gave white cubic-crystals of (*R*)-heliphos. (*S*)-heliphos ((*S*)-15) was obtained by the same procedure from (*S*)-11.

Heliphos and its precursors were characterized by ^1H , ^{13}C , ^{31}P NMR spectroscopy, MS (mass spectroscopy), and elemental analysis. The $^{31}\text{P}\{^1\text{H}\}$ NMR spectrum of heliphos recorded in CDCl_3 solution contained three singlets at -12.2, -21.7, and -24.1 ppm. ^1H NMR signals of the framework methylene protons were broadened by coupling with phosphorus. The optical rotation of (*R*)-heliphos was -71.7 (at 589 nm, toluene, c 1.0174), and it was +72.5 (at 589 nm, toluene, c 0.5310) for (*S*)-heliphos. Enantiomeric purities of the bis(phosphine) phosphine oxide ((*R*)-14, (*S*)-14) were confirmed by ^{31}P NMR analysis after adding optically pure (*R*)-(+)-1,1'-bi-2-naphthol in C_6D_6 solution.³⁰ For example, a phosphorus signal of (*R*)-14 at 32.6 ppm will shift to low field and separate into two peaks after adding optically pure (*R*)-(+)-1,1'-bi-2-naphthol if (*R*) and (*S*)-14 is not optically pure. This shift may be explained by an acid-base interaction between the OH groups of (*R*)-(+)-1,1'-bi-2-naphthol and the P=O groups of (*R*)-14. The optical purity of heliphos was determined by the same method after oxidizing heliphos to heliphos trioxide with a 10% aqueous solution of hydrogen peroxide.

2.3 Synthesis and Characterization of [(heliphos)Rh(NBD)](ClO₄)

The rhodium complex [(heliphos)Rh(NBD)](ClO₄) ((*R*)-16 and (*S*)-16) was prepared by mixing [Rh(NBD)₂](ClO₄) and heliphos in a CH₂Cl₂ solution (scheme 2.10).



Scheme 2.10

The complex was air-stable in the solid state and in solution as well. Both enantiomers were characterized by ¹H, ¹³C, ³¹P NMR spectroscopy and elemental analysis. The structure of the (*R*)-heliphos rhodium complex was confirmed by X-ray crystallography, and the solid-state structure is shown in figure 2.1. Pertinent structural information can be found in tables 2.2 through 2.4.

The ³¹P{¹H} NMR spectrum in CD₂Cl₂ showed three sets of resonances which corresponded to the three coordinated inequivalent phosphorus atoms in [(heliphos)Rh(NBD)](ClO₄). The spectrum (figure 2.2) appeared as an AEMX spin system with large Rh-P coupling constants and small P-P coupling constants. The three Rh-P coupling constants were 111.6, 113.9, 116.7 Hz. These constants are close to those reported for other tripodal phosphine rhodium complexes.^{19, 20}

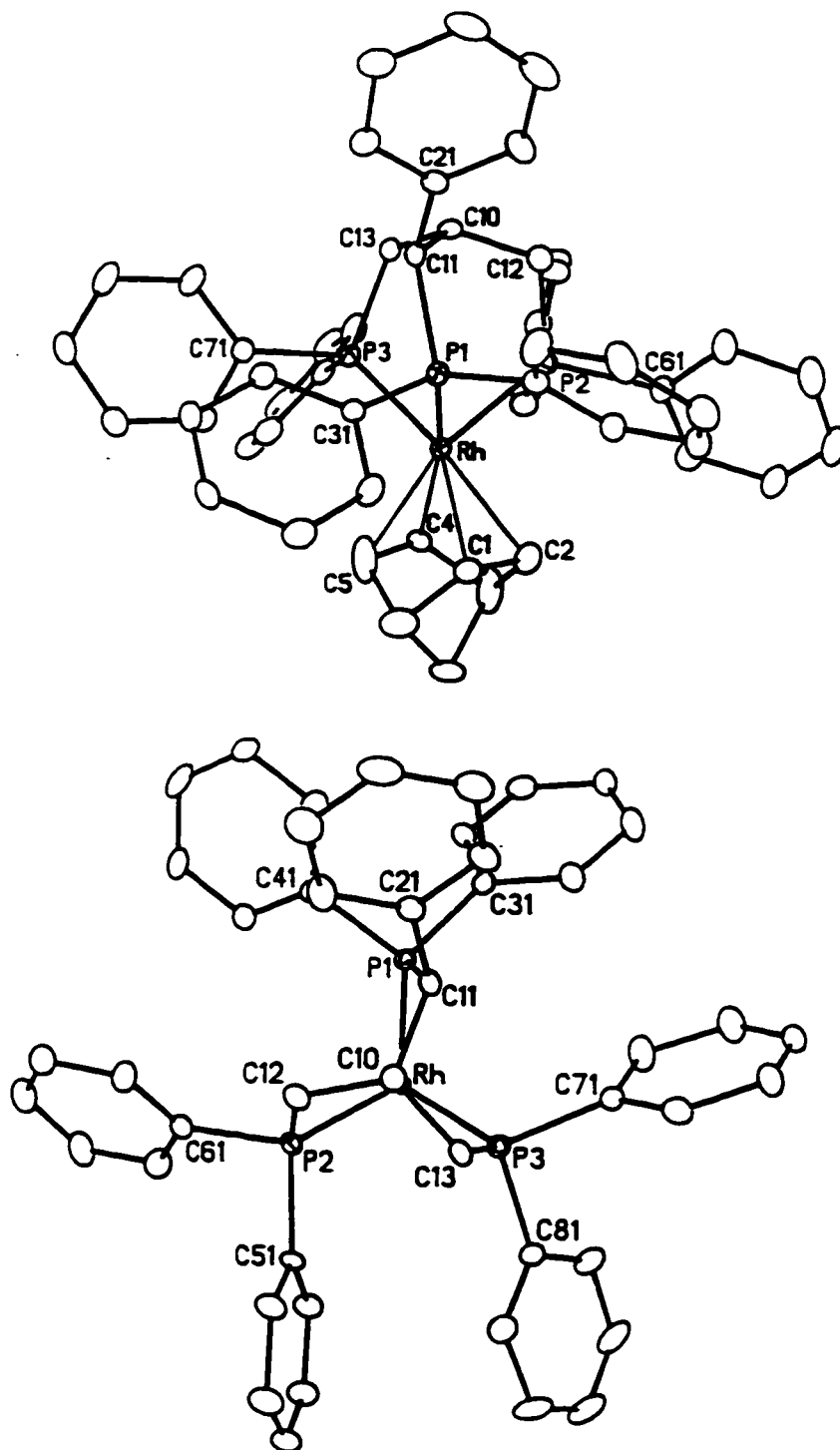


Figure 2.1 (Top) The molecular structure of the cationic portion of $[(R)\text{-heliphos})\text{Rh}(\text{NBD})](\text{ClO}_4)$. Hydrogen atoms have been omitted for clarity. (Bottom) View looking down the crystallographic *pseudo*- C_3 axis. NBD has been omitted for clarity.

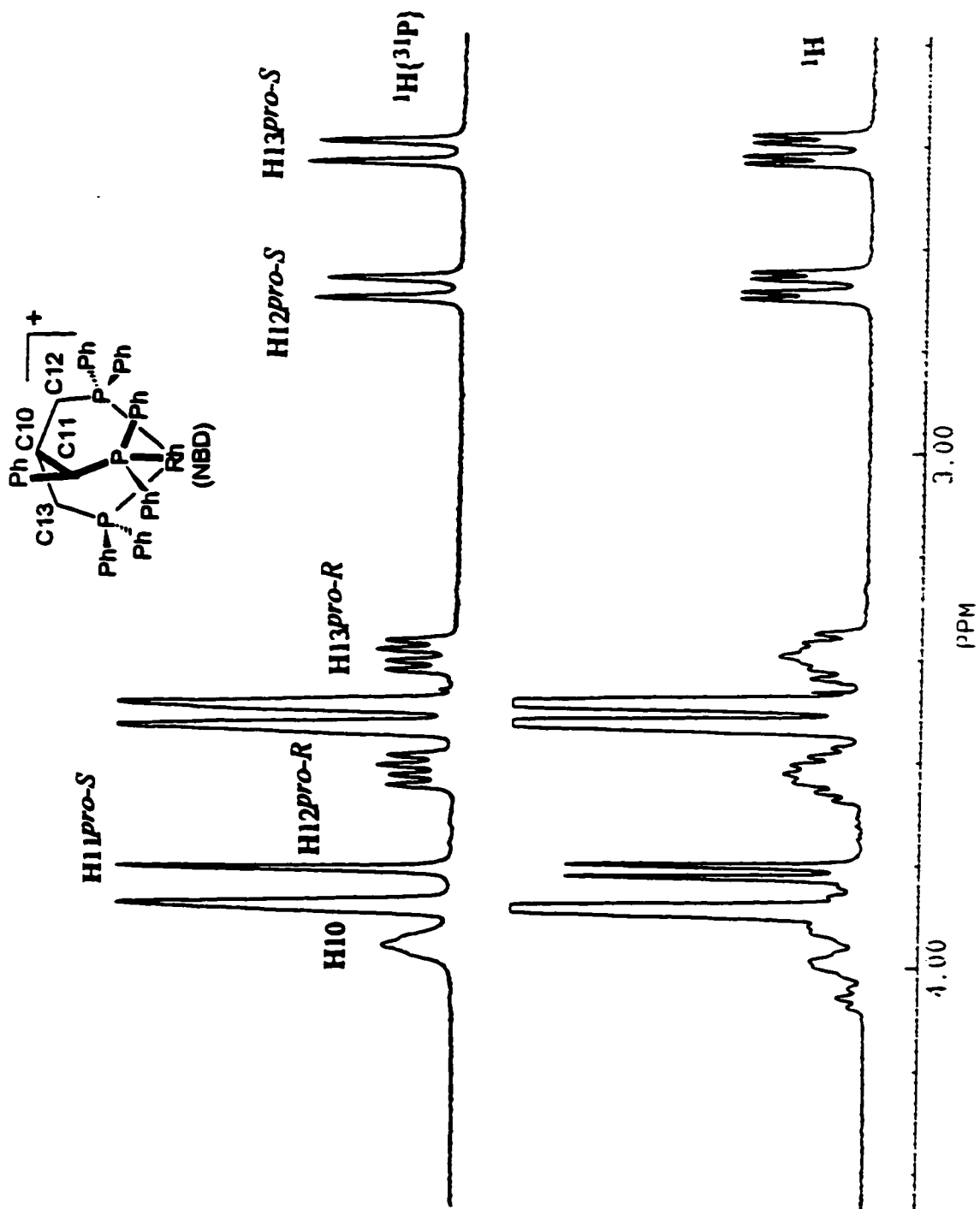


Figure 2.2 $^{31}\text{P}\{^1\text{H}\}$ NMR spectrum of $[(\text{heliphos})\text{Rh}(\text{NBD})](\text{ClO}_4)$ in CD_2Cl_2 at r.t.

The ^1H NMR spectrum recorded in CD_2Cl_2 was poorly resolved in due to overlap of the signals from NBD by those of tripodal framework methylene protons. By using a 1:1, CD_2Cl_2 : CD_3Cl mixed solvent system, the 3.3-4.0 ppm region of the ^1H NMR spectrum was well resolved as shown in figure 2.3. In order to obtain all geminal and vicinal coupling constants, the $^1\text{H}\{^{31}\text{P}\}$ NMR spectrum was recorded. COSY and NOE difference experiments were performed to assign the signals of all framework protons. It was found that three resonances at 3.80, 2.68, 2.42 ppm did not couple to the apical proton and appeared as either a singlet or as a doublet in the $^1\text{H}\{^{31}\text{P}\}$ spectrum. In contrast, the two resonances at 3.63 and 3.40 ppm coupled with the apical proton and appeared as a doublet of doublets. From NOE difference spectrum, ~ 6% NOE for the signal at 3.81 ppm and 25% NOE for the signal at 2.40 ppm were observed if the peak at 3.38 ppm was irradiated, and ~ 4% NOE for the signal at 2.40 ppm and 30% NOE for the signal at 2.68 ppm was observed if the peak at 3.62 ppm was irradiated. On the basis of these data, the framework protons were assigned as shown in table 2.1 and in figure 2.3.

Table 2.1 ^1H NMR data of framework protons of $[(\text{heliphos})\text{Rh}(\text{NBD})](\text{ClO}_4)$.

Signal (ppm)	Assignment	H-H coupling constant(Hz)
3.98 (m)	H10	-
3.80 (s)	H11 $_{pro-S^*}$	$^3J = 0$
3.63 (d,d)	H12 $_{pro-R}$	$^2J = 15.6$, $^3J = 7.6$
3.40 (d,d)	H13 $_{pro-R}$	$^2J = 16.2$, $^3J = 7.0$
2.68 (d)	H12 $_{pro-S}$	$^2J = 15.6$, $^3J = 0$
2.42 (d)	H13 $_{pro-S}$	$^2J = 16.2$, $^3J = 0$

* $Pro-S(R)$: assuming replacement by a phenyl ring

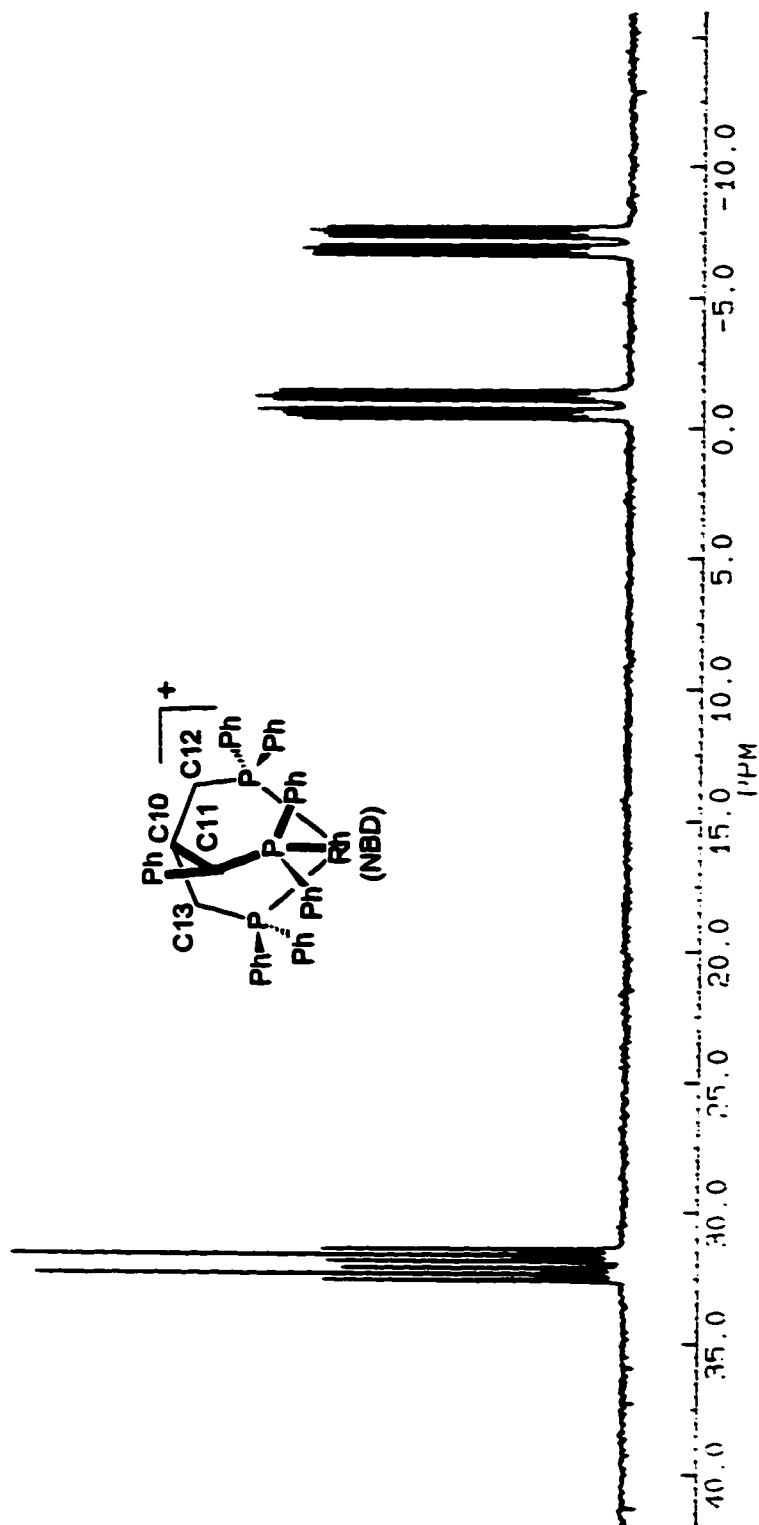


Figure 2.3 ^1H (Bottom) and $^1\text{H}\{^{31}\text{P}\}$ (Top) NMR spectrum of framework protons region of $[(\text{heliphos})\text{Rh}(\text{NBD})](\text{ClO}_4)$ in $\text{CD}_2\text{Cl}_2/\text{CDCl}_3$ (1:1).

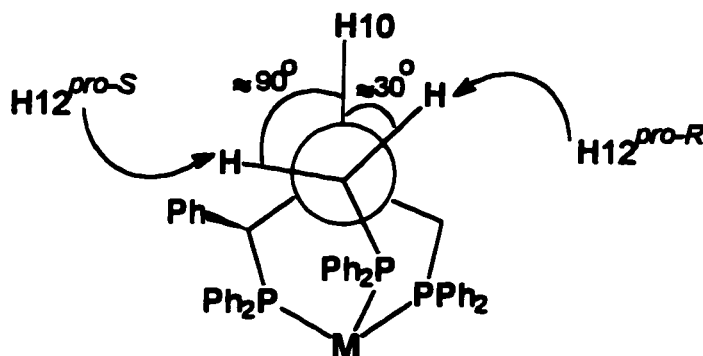
The optical rotations for the enantiomers of [(heliphos)Rh(NBD)](ClO₄) were significantly higher than the corresponding free ligands (+127.18° (toluene, *c* 0.5032, *R*) and -128.64° (toluene, *c* 0.4975, *S*)).

2.4 Solid-State and Solution Conformational Study of [((*R*)-heliphos)Rh(NBD)](ClO₄)

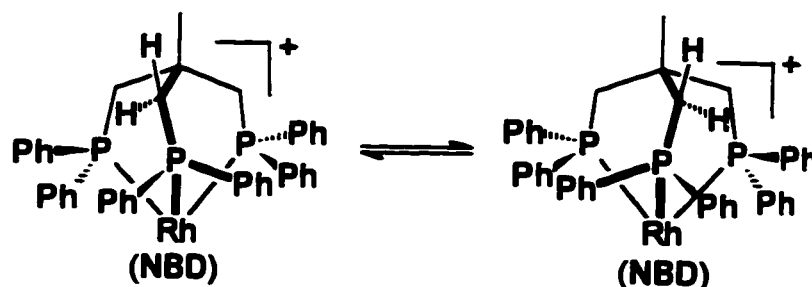
The crystal structure of Λ -[Rh((*R*)-heliphos)(NBD)](ClO₄) showed that (*R*)-heliphos adopted the predicted Λ -conformation in the solid-state with the Rh-P-C(methylene)-C10 torsional angles ranging from 35.1(7)° through 27.9(6)°. These values are comparable to those observed for other tripodal phosphine metal complexes.^{20, 21} The rhodium phosphine bond lengths (2.352, 2.376, 2.308 Å) also are comparable to analogous tripodal phosphine complexes. The distances (in Å) from the plane defined by the phosphorus atoms and the *ipso*-carbons of the axial phenyl groups were 0.474(8), 0.372(9), and 0.415(9). The corresponding distances for the equatorial phenyl groups were -0.21(8), -0.168(9), and -0.107(8) (inclinations towards the ligand framework are assigned a negative value). The pendant phenyl groups were in the predicted asymmetric array around the metal centre.

Solution NMR studies suggested that the framework of [Rh((*R*)-heliphos)(NBD)](ClO₄) also strongly favored the Λ -conformer in solution for two reasons. First, the pro-*S* protons at C12 and C13 of Λ -(*R*)-heliphos are oriented towards the equatorial phenyl group in the adjacent arm's phosphine. This orientation is similar to that of the framework phenyl group in the unfavored Δ -(*R*)-heliphos. For both C12, and C13 the ¹H{³¹P} NMR signal for the pro-*S* proton was shifted upfield from the pro-*R* proton by ~0.9 ppm. I propose that these differences in chemical shift were caused by ring current effects of the equatorial phenyl groups, and indicate that interconversion with appreciable amounts of Δ -(*R*)-heliphos did not occur in solution. Second, the coupling

constants between the apical proton at C10 and the *pro-S* methylene protons at C11, C12 and C13 were all ~ 0 Hz, while those with the *pro-R* methylene protons at C12 and C13 were ~ 7 Hz. According to the Karplus relationship,³¹ a coupling constant equal to 0 Hz corresponds to a H-C(10)-C(methylene)-H dihedral angle of 90° . As shown below, molecular models predict the H10-H^{*pro-S*} dihedral angles will be $\sim 90^\circ$ in Λ -(*R*)-heliphos. Further, these angles are supported by those obtained from the calculated hydrogen atoms in the crystal structure of [Rh(*R*-heliphos)(NBD)](ClO₄) (H10-H11^{*pro-S*} = 87° , H10-H12^{*pro-S*} = 82° , H10-H13^{*pro-S*} = 75°).³² The relatively large diastereotopic shift difference between *pro-S* and *pro-R* of framework methylene protons along with the difference in ³J for H^{*pro-S*}-H10 and H^{*pro-R*}-H10 values indicated that the heliphos-rhodium cage is locked in one conformation.



In contrast, interconversion between Λ - and Δ -triphos was shown to occur by the following experiment. The ¹H NMR spectrum of [Rh(triphos)(NBD)](ClO₄)³³ in CD₂Cl₂ solution was measured. The methylene protons in coordinated triphos (CH₃C(CH₂P(Ph)₂)₃) are diastereotopic, and as shown below, they exchange magnetic environments upon interconversion between the Λ - and Δ -conformers.



Scheme 2.11

The signals for the methylene protons at $-80\text{ }^{\circ}\text{C}$ were indistinguishable, indicating that interconversion between Λ - and Δ -[Rh(triphos)(NBD)](ClO₄) was rapid in solution. Further, the signals for the methylene protons in the published ¹H NMR spectrum of [Fe(CH(CH₂PPh₂)₃)(MeCN)₃](BPh₄)₂ coincide,^{26b} and the H(apical) - H(methylene) coupling constant was $\sim 4\text{ Hz}$. This suggests that the framework of [Fe(CH(CH₂PPh₂)₃)(MeCN)₃](BPh₄)₂ rapidly interconverted between the Λ - and Δ -conformers in solution, and that the chemical shift and coupling constant of the methylene signal were averaged over the two environments.

2.5 Conclusion

An efficient procedure to synthesize optically pure (*R*)- and (*S*)-heliphos has been developed. The stereogenic carbon in heliphos dictated which conformer was adopted by the coordinated ligand. Coordinated (*R*)-heliphos adopted the predicted Λ -conformer in the solid state, and NMR experiments showed that its conformation was rigid in solution as well. Both molecular models and models based on the crystal structure of Λ -[Rh((*R*)-heliphos)(NBD)](ClO₄) show that the framework phenyl group and the *syn* equatorial phenyl group would physically overlap in the unfavored Δ -conformer.

Crystal structure of [Rh((*R*)-heliphos)(NBD)](ClO₄)

Crystals suitable for analysis by x-ray diffraction were obtained by slow evaporation of solutions of [Rh((*R*)-heliphos)(NBD)](ClO₄) in methanol under a stream of argon gas. The X-ray structure determination was performed by Dr. Robert McDonald at the Structure Determination Laboratory, University of Alberta.

Data were measured using a Enraf-Nonius CAD4 diffractometer with Mo K α radiation ($\lambda = 0.71073 \text{ \AA}$; maximum $2\theta = 50.0^\circ$); 8169 independent reflections (7116 with $I > 2\sigma(I)$) were measured. The structure was solved via direct methods (*DIRDIF-94*). Full-matrix, least-squares refinement on F^2 (*SHELXL-93*) yield $R_1 = 0.0579$ ($I > 2\sigma(I)$), and $wR_2 = 0.1567$.

Table 2.2 provides relevant collection and refinement data. Relevant bond distances and bond angles are provided in table 2.3 and 2.4.

Table 2.2 Crystallographic Data for [Rh((*R*)-heliphos)(NBD)](ClO₄)

formula	C₅₄H₅₃ClO₅P₃Rh
formula weight	1013.23
crystal dimensions (mm)	0.23 x 0.25 x 0.24
crystal system	monoclinic
space group	P2₁ (No. 4)
unit cell parameters	
a (Å)	9.5295(9)
b (Å)	18.307(2)
c (Å)	13.564(2)
β (deg)	99.362(13)
V (Å³)	2334.9(5)
Z	2
ρ_{calcd} (g cm⁻³)	1.441
μ (mm⁻¹)	0.575
scan type	θ-2θ
data collection 2θ limit (deg)	50.0
total data collected	8826 (-11 ≤ h ≤ 11, -21 ≤ k ≤ 21, -16 ≤ l ≤ 16)
independent reflections	8169
number of observations	7116 (F₀² > 2σ(F₀²))
final R indices	
F₀² > 2σ(F₀²)	R₁ = 0.0579, ωR₂ = 0.1567
all data	R₁ = 0.0706, ωR₂ = 0.1715
largest difference peak and hole	1.488 and -0.987 e Å⁻³

Table 2.3 Bond distances (Å) for [Rh((*R*)-heliphos)(NBD)](ClO₄)

bond	distance	bond	distance
Rh-P1	2.352(2)	P3-C71	1.831(8)
Rh-P2	2.376(2)	P3-C81	1.830(7)
Rh-P3	2.308(2)	C1-C2	1.426(14)
Rh-C1	2.216(7)	C1-C6	1.55(2)
Rh-C2	2.254(10)	C2-C3	1.446(15)
Rh-C4	2.177(7)	C3-C4	1.480(14)
Rh-C5	2.260(13)	C3-C7	1.584(9)
P1-C11	1.867(8)	C4-C5	1.376(14)
P1-C31	1.826(8)	C5-C6	1.44(2)
P1-C41	1.830(7)	C6-C7	1.49(2)
P2-C12	1.849(9)	C10-C11	1.574(11)
P2-C51	1.831(8)	C10-C12	1.550(11)
P2-C61	1.851(7)	C10-C13	1.545(10)
P3-C13	1.841(9)	C11-C21	1.522(10)

Numbers in parentheses are estimated standard deviations

Table 2.4 Bond angles (deg) for [Rh(*R*-heliphos)(NBD)](ClO₄)

Interatomic Angle	Angle	Interatomic Angle	Angle
P1-Rh-P2	91.71(8)	C11-P1-C31	105.5(3)
P1-Rh-P3	89.21(7)	C11-P1-C41	108.6(3)
P1-Rh-C1	90.0(3)	C31-P1-C41	98.0(4)
P1-Rh-C2	112.4(3)	Rh-P2-C12	107.2(3)
P1-Rh-C4	159.6(2)	Rh-P2-C51	116.4(3)
P1-Rh-C5	124.4(3)	Rh-P2-C61	121.1(3)
P2-Rh-P3	88.43(6)	C12-P2-C51	107.2(4)
P2-Rh-C1	122.0(2)	C12-P2-C61	103.2(4)
P2-Rh-C2	90.8(3)	C51-P2-C61	100.5(4)
P2-Rh-C4	108.0(2)	Rh-P3-C13	110.6(2)
P2-Rh-C5	143.8(3)	Rh-P3-C71	118.2(3)
P3-Rh-C1	149.6(2)	Rh-P3-C81	117.6(2)
P3-Rh-C2	158.4(3)	C13-P3-C71	105.4(3)
P3-Rh-C4	96.0(2)	C13-P3-C81	105.1(4)
P3-Rh-C5	94.0(3)	C71-P3-C81	98.4(3)
C1-Rh-C2	37.2(4)	Rh-C1-C2	72.9(5)
C1-Rh-C4	75.6(4)	Rh-C1-C6	97.9(6)
C1-Rh-C5	62.0(4)	Rh-C2-C1	70.0(5)
C2-Rh-C4	63.8(4)	Rh-C2-C3	93.6(6)
C2-Rh-C5	74.3(4)	Rh-C4-C3	95.8(6)
C4-Rh-C5	35.8(4)	Rh-C4-C5	75.4(6)
Rh-P1-C11	110.2(2)	Rh-C5-C4	68.8(6)
Rh-P1-C31	115.8(2)	Rh-C5-C6	99.4(7)
Rh-P1-C41	117.5(3)	C11-C10-C12	115.0(6)

Interatomic Angle	Angle	Torsional Angle	Angle
C11-C10-C13	111.5(6)	Rh-P1-C11-C10	-30.6(6)
C12-C10-C13	114.7(6)	Rh-P2-C12-C10	-35.1(7)
P1-C11-C10	112.0(5)	Rh-P3-C13-C10	-27.9(6)
P1-C11-C21	118.6(5)		
C10-C11-C21	11.4(6)		
P2-C12-C10	114.8(6)		
P3-C13-C10	114.7(5)		

Numbers in parentheses are estimated standard deviations

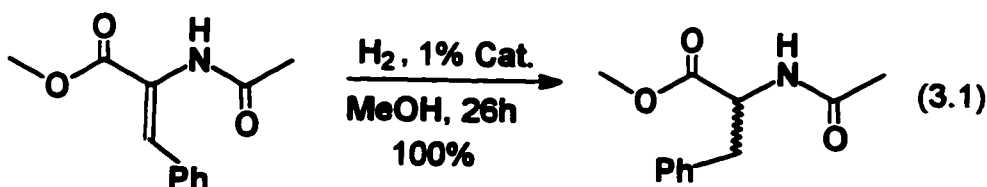
Chapter 3

Catalysis

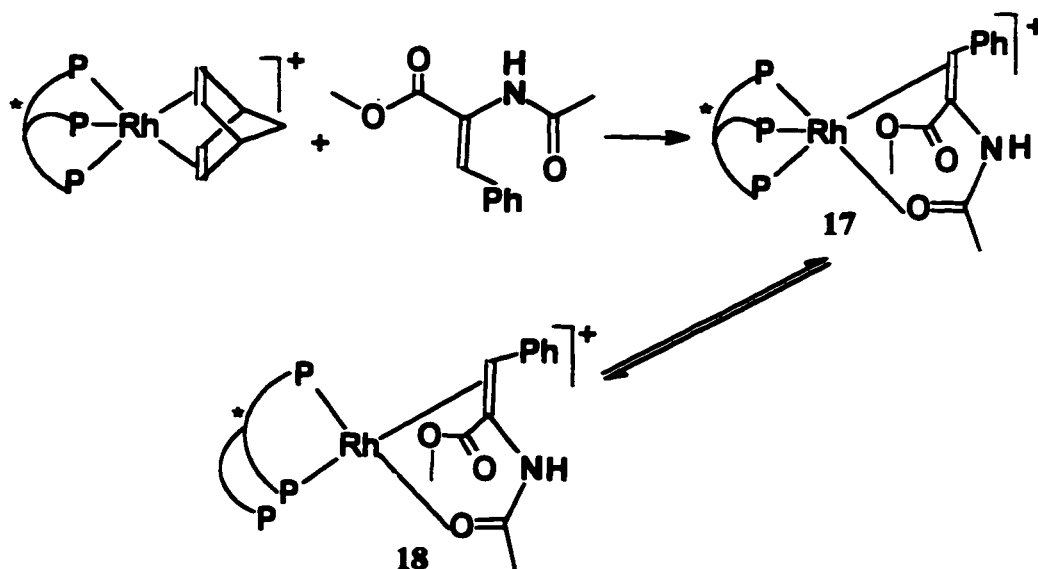
3.1 Catalytic Reactions

Cationic rhodium(I) phosphine complexes are known to be active catalysts for hydrogenation⁵, hydroboration³⁴, hydroacylation⁵, and hydrosilylation³⁵ reactions. Therefore, [(heliphos)Rh(NBD)](ClO₄) was assessed as a catalyst precursor for several of these reactions.

Asymmetric hydrogenation is among the most developed catalytic reactions to date. The most successful catalysts are rhodium- or ruthenium-bis(phosphine) complexes. The first enantioselective catalytic hydrogenation using a chiral tripodal phosphine as ligand was reported by Burk.¹¹ The same substrate used by Burk was hydrogenated using [(heliphos)Rh(NBD)](ClO₄) as a catalyst precursor (eq. 3.1).



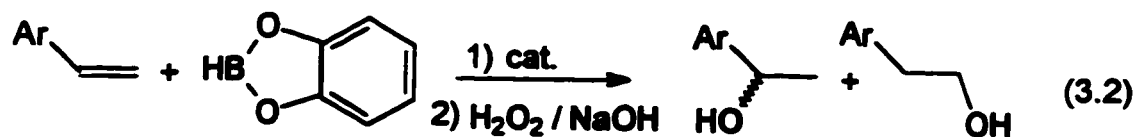
Methyl (Z)- α -acetamidocinnamate was hydrogenated in methanol at 25 °C and at 4 atm of H₂ to give the product, methyl 2-acetamido-3-phenylpropanoate in 12.3% ee. This low ee suggests that the heliphos-Rh(I) catalyst suffered the same problem as Burk's catalyst, phosphine arm dissociation as shown in scheme 3.1. The intermediate 17 is coordinatively saturated and dissociation of one arm of heliphos to form 18 is required prior to reaction with dihydrogen.



Scheme 3.1

The helicity of the framework will be destroyed if phosphine arm dissociation occurs, causing the catalyst to lose conformational rigidity. It was expected that by using monodentate substrates such as acetophenone, arm dissociation could be avoided. Unfortunately, this catalyst was inactive towards hydrogenation of acetophenone even at 85 atm of hydrogen pressure.

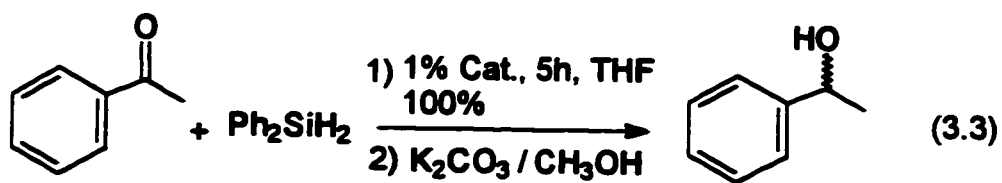
The asymmetric hydroboration of styrene by catecholborane was also investigated (eq. 3.2).



Reaction of styrene with catecholborane in THF at 25 °C for 4 hours in the presence of 1% catalyst followed by oxidation gave 93% yield of 1-phenylethanol and 7% yield of 2-

phenylethanol. This regioselectivity is close to those reported in the literature for bisphosphine-Rh(I) catalyst. Unfortunately, the ee of 1-phenylethanol was 0%.

The asymmetric hydrosilylation of acetophenone by diphenylsilane also was investigated (eq. 3.3).



The hydrosilylation was attempted both at room temperature and at -30°C . The reaction was found to proceed only at room temperature, and then with 0% ee.

3.2 Conclusion

Attempts to use $[\text{Rh}((R)\text{-heliphos})(\text{NBD})](\text{ClO}_4)$ as an enantioselective catalyst appear to be hampered by phosphine arm dissociation. Arm dissociation is a well-documented process for 18-electron, rhodium-(I)-tripodal phosphine compounds.^{19a, 36} To avoid this problem, it was necessary to design and synthesize a catalyst in which the metal centre prefers octahedral geometries.

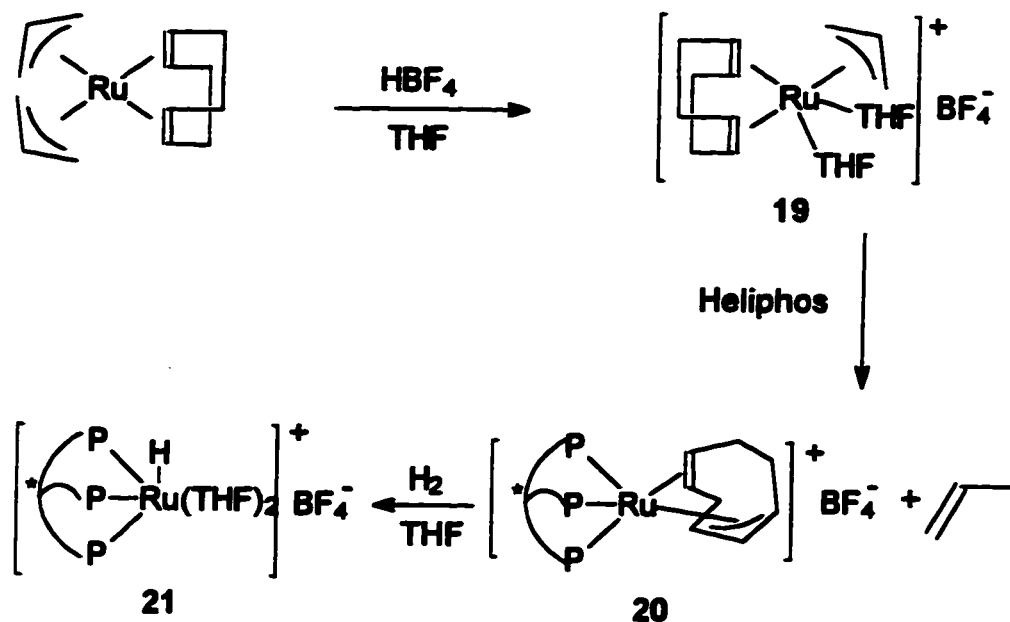
Chapter 4

Ruthenium Compounds of Heliphos

4.1 Synthesis

Ruthenium phosphine chemistry has drawn great attention since the pioneering work by Saburi and Noyori on the use of chiral Ru(II) complexes as catalysts for asymmetric hydrogenation.⁵ The Noyori group has demonstrated the remarkable catalytic enantioselectivities of a series of BINAP-Ru(II) complexes.⁵ It is likely that octahedral intermediates are involved in Ru(II) catalyzed reactions³⁷ because the Ru(II) d⁶ metal centre prefers octahedral geometry. Phosphine arm dissociation from tripodal phosphine-Ru(II) compounds is therefore unlikely to occur. Compound 21 (scheme 4.1) was targeted as a potential catalyst for the following reasons. First, the solvento ligands (eg. THF, MeOH, or (CH₃)₂CO) were chosen to be labile, allowing for easy displacement by the substrate. Second, it is likely that the hydrido ligand will undergo facile insertion reactions. Third, hydride insertion will generate the equivalent of a vacant coordination site, allowing for further reactions during the catalytic cycle. Compound 21 therefore will possess the equivalent of 3 vacant coordination sites. The following routes to generate compounds 21 were investigated.

Route A. The protonation of Ru(COD)(η^3 -C₃H₅)₂ by HBF₄ in acetonitrile removed an allyl group to generate the bis(solvento) cation which is known to react with BINAP to produce an active catalyst precursor. This chemistry was developed in this lab.³⁸ It was expected that Ru(COD)(η^3 -C₃H₅)₂ would be protonated by HBF₄ in THF to generate the bis(THF) cation 19 which would then react with heliphos to form compound 20. The proposed reaction pathway is outlined in scheme 4.1.

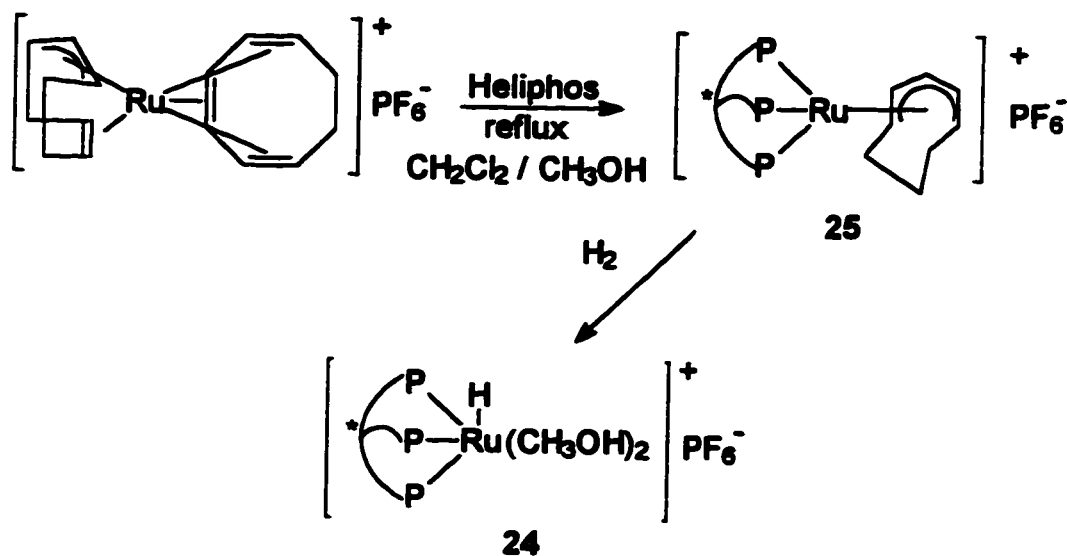


Scheme 4.1

Hydrogenation of compound **20** was expected to generate the active catalyst **21**. The products of the reaction between heliphos and **19** were fluxional at room temperature. Low temperature ($-40\text{ }^{\circ}\text{C}$) ^{31}P NMR spectra indicated that approximately 40% of the products contained tridentate coordinated heliphos, showing three *pseudo*-triplets at 42.1 ($J = 32\text{ Hz}$), 14.9 ($J = 32\text{ Hz}$), -2.4 ($J = 32\text{ Hz}$) ppm. The remaining products contained bidentate coordinated heliphos. Unfortunately, this mixture could not be separated. Attempts to improve the yield of tridentate product by changing the solvent and temperature were not successful.

Route B. The hydrido diene complex $[(\text{triphos})\text{RuH}(\text{COD})](\text{PF}_6)$ is known.³⁹ Treatment of $[\text{RuH}(\text{COD})(\text{NH}_2\text{NMe}_2)_3](\text{PF}_6)$ (in CH_3OH) with triphos (in CH_2Cl_2) at $0\text{ }^{\circ}\text{C}$ gives the compound $[(\text{triphos})\text{RuH}(\text{COD})](\text{PF}_6)$ which converts irreversibly to the η^3 -cyclooctenyl complex $[(\text{triphos})\text{Ru}(\eta^3\text{-C}_8\text{H}_{11})](\text{PF}_6)$ above room temperature. The heliphos analogs (**22**, **23**) were expected to be prepared by the procedure shown in scheme 4.2.

between heliphos and $[\text{Ru}(1,3:5,6\text{-}\eta\text{-C}_8\text{H}_{11})(\eta^6\text{-}1,3,5\text{-C}_8\text{H}_{10})](\text{PF}_6)$ was attempted. Heliphos is not very soluble in CH_3OH , so the reaction conditions were modified as illustrated in scheme 4.3.



Scheme 4.3

In contrast to the reaction with monophosphines, $[\text{Ru}(1,3:5,6\text{-}\eta\text{-C}_8\text{H}_{11})(\eta^6\text{-}1,3,5\text{-C}_8\text{H}_{10})](\text{PF}_6)$ did not react with heliphos in $\text{CH}_3\text{OH}/\text{CH}_2\text{Cl}_2$ to give the expected heliphos ruthenium complex 25. When the reaction mixture refluxed for one day in acetone, many uncharacterized species were observed.

4.2 Conclusion

Transition metal complexes containing triphos are numerous and constitute an important class of organometallic compounds. While the newly developed chiral tripodal phosphine heliphos seems unwilling to follow the chemistry of triphos, the reason why heliphos does not show the same coordinating ability is not clear. It is unlikely that the steric or electronic effects of the phenyl ring at the stereogenic centre in heliphos

weakened the coordinating ability of heliphos. Further investigation is necessary to determine which factors govern the coordinating ability of these ligands.

Experimental Section

Instrumentation

All ^1H , ^{13}C , and ^{31}P NMR spectra were measured with a Bruker AM-400 NMR spectrometer operating at 400.13 MHz, 100.61 MHz, and 161.97 MHz respectively. ^1H and ^{13}C NMR chemical shifts are reported in parts per million (δ) relative to tetramethylsilane using the solvent as an internal reference. ^{31}P NMR chemical shifts are reported in parts per million (δ) relative to an 85 % H_3PO_4 external reference. Mass spectra were measured using Kratos ms50 or AEI ms9 mass spectrometers. Microanalyses were performed at the University of Alberta Microanalysis Laboratory. Optical rotations were measured with a Perkin-Elmer 241 polarimeter at 589 nm (sodium D line) using 1.0 dm cells. Specific rotations, $[\alpha]_{\text{D}}$, are reported in degrees per decimeter at 25 °C, and the concentration (c) is given in grams per 100 mL. Melting points were measured with a Gallenkamp capillary melting point apparatus and are uncorrected.

Starting materials and reagents

The solvents *n*-hexane (K, Ph_2CO), methylene chloride (CaH_2), tetrahydrofuran (K, Ph_2CO), diethyl ether (K, Ph_2CO), toluene (K, Ph_2CO), triethylamine (CaH_2), tributylamine (CaH_2), and xylenes (CaH_2) were distilled from drying agents under argon, except methanol which was deoxygenated by bubbling argon or nitrogen for 1 h. The argon and dinitrogen gases were passed through a bed of Drierite drying agent. Unless stated otherwise, commercial reagents were used without further purification and all operations were performed under an inert atmosphere of argon or dinitrogen gas.

Styrene, acetophone, diphenylsilane, phenylsilane, and catecholborane were distilled before use. (*Z*)-methyl- α -acetamidocinnamate,⁴¹ (*R*)-(+)- α -methoxy- α -(trifluoromethyl)phenylacetyl chloride (Mosher's acid chloride), Mosher's ester,⁴² dimethylmalonate,⁴³ [Rh(NBD)₂](ClO₄),⁴⁴ [HRu(COD)(NH₂NMe₂)₃](PF₆),³⁹ [Ru(COD)(η^3 -C₃H₅)₂],⁴⁵ and [Ru(1-3:5,6- η -C₈H₁₁)(η^6 -1, 3, 5-C₈H₁₀)](PF₆)⁴⁰ were prepared according to published literature methods.

CH₃CH(PPh₂)CH(COOC₂H₅)₂ (1)

A solution of diethyl ethylidenemalonate (2.00 mL, 10.90 mmol) and diphenylphosphine (2.00 mL, 11.50 mmol) in CHCl₃ (30 mL) was stirred at room temperature for 3 h. The mixture was concentrated under reduced pressure to afford a colorless liquid product **1** quantitatively by ¹H NMR analysis. ¹H NMR (CDCl₃) δ 1.12 (dd, *J* = 4.5, 11.3 Hz, 3 H), 1.25 (m, 6 H), 3.16 (m, 1 H), 3.32 (t, *J* = 7.0 Hz, 1 H), 4.12 (m, 2 H), 4.20 (m, 2 H), 7.35 (m, 6 H), 7.51 (m, 4 H); ¹³C NMR (CDCl₃) δ 13.71, 13.94, 30.36 (d, *J*_{P-C} = 14.8 Hz), 54.32 (d, *J*_{P-C} = 21.1 Hz), 61.07, 61.26, 126.15, 128.28, 128.38, 128.60, 128.66, 129.14, 130.43, 130.64, 132.40, 132.76, 133.14, 133.94, 134.36, 181.60; ³¹P NMR (CDCl₃) δ -3.59.

CH₃CH[P(O)Ph₂]CH(CH₂OH)₂ (3)

To a stirred mixture of LiAlH₄ (1.20 g, 31.60 mmol) and ether (50 mL) was added dropwise a solution of **1** (obtained from previous reaction without purification) (4.20 g, 10.90 mmol) in ether (10 mL) at 0 °C for 10 min. The dropping funnel was rinsed with ether (10 mL), the reaction mixture was stirred for 20 min at 0 °C, and then for 20 min at room temperature. The LiAlH₄ was neutralized by the dropwise addition of 1.2 g of deoxygenated distilled water, 1.2 g of deoxygenated 10% NaOH solution at 0 °C, and 3.6 g of deoxygenated distilled water at room temperature. The mixture was stirred for 30

min, filtered, washed with ether (3 x 20 mL), and concentrated under reduced pressure yielding phosphine-diol 2. This phosphine-diol 2 could be purified by recrystallization from toluene at 0 °C. For 2: $^1\text{H NMR}$ (CDCl_3) δ 0.91 (dd, $J = 7.2, 13.19$ Hz, 3 H), 1.84 (m, 1 H), 2.64 (m, 1 H), 3.70 (m, 2 H), 3.91 (dd, $J = 7.26, 10.74$ Hz, 1 H), 4.01 (dd, $J = 3.86, 10.74$ Hz, 1 H), 7.20-7.60 (m, 10 H); $^{31}\text{P NMR}$ (CDCl_3) δ -6.80.

The crude 2 was dissolved in CH_2Cl_2 (50 mL, undistilled) and oxidized by adding a solution of 10 % H_2O_2 (20 mL). The reaction mixture was stirred for 10 min and then washed with a solution of saturated $\text{Na}_2\text{S}_2\text{O}_3$ (20 mL) until the excess H_2O_2 was neutralized (negative result with saturated solution of KI). The organic layer was dried over Na_2SO_4 , filtered, and concentrated under reduced pressure affording 3 in 74.2 % yield (2.42 g), as an oily solid. Further purification was unnecessary: $^1\text{H NMR}$ (CDCl_3) δ 1.12 (dd, $J = 7.5, 17.1$ Hz, 3 H), 2.29 (m, 1 H), 3.02 (m, 1 H), 3.16 (br, 1 H), 3.39 (m, 2 H), 3.62 (m, 2 H), 5.10 (br, 1 H), 7.49 (m, 6 H), 7.85 (m, 4 H); $^{13}\text{C NMR}$ (CDCl_3) δ 7.54, 30.67 (d, $J_{\text{P-C}} = 71.2$ Hz), 43.67, 59.85, 61.77 (d, $J_{\text{P-C}} = 11.9$ Hz), 128.74, 128.85, 128.97, 130.86, 130.96, 131.05, 131.08, 131.89; $^{31}\text{P NMR}$ (CDCl_3) δ 41.04.

$\text{CH}_3\text{CH}[\text{P}(\text{O})\text{Ph}_2]\text{CH}(\text{CH}_2\text{OMe})_2$ (4)

To a solution of 3 (1.00 g, 3.28 mmol) and dry triethylamine (1.50 mL, 10.76 mmol) in CH_2Cl_2 (20 mL) at - 35 °C was added a solution of methanesulfonyl chloride (0.62 mL, 8.01 mmol) in dry CH_2Cl_2 (10 mL) over 10 min. The mixture was allowed to warm to room temperature over 1 h, and then stirred for an additional 45 min. In air, the reaction flask was placed in an ice bath and the solution was quenched by the addition of crushed ice (8 g), followed by cold water (8 g) with vigorous stirring. The ice bath was removed, and the solution stirred until the ice melted. The organic layer was separated, and the aqueous layer back-extracted with CH_2Cl_2 (20 mL). The combined organic layers were sequentially washed with cold water (2 x 10 mL), cold saturated NaHCO_3 (2 x 10

mL), and cold brine (2 x 10 mL). The organic layer was dried over Na_2SO_4 , filtered, and concentrated under reduced pressure to afford a light-yellow oily solid **4** in 84.9 % yield (1.41 g): ^1H NMR (CDCl_3) δ 1.15 (dd, $J = 6.7, 16.5$ Hz, 3 H), 2.57 (br, 1 H), 2.82 (m, 1 H), 3.00 (s, 3 H), 3.03 (s, 3 H), 4.34 (m, 3 H), 4.80 (dd, $J =$ Hz), 7.51 (m, 6 H), 7.82 (m, 4 H); ^{13}C NMR (CDCl_3) δ 8.04, 30.41 (d, $J_{\text{P-C}} = 70.2$ Hz), 36.99, 37.36, 37.51, 67.47, 68.34 (d, $J_{\text{P-C}} = 11.5$ Hz), 128.88, 129.01, 129.11, 129.23, 130.09, 130.21, 130.65, 130.73, 130.81, 131.04, 131.18, 132.17, 132.39; ^{31}P NMR (CDCl_3) δ 36.73.

$\text{CH}_3\text{CH}[\text{P}(\text{O})\text{Ph}_2]\text{CH}(\text{CH}_2\text{PPh}_2)_2$ (5**)**

Potassium hydride (0.386 g, 3.36 mmol, 35% mineral oil dispersion) was washed with THF (3 x 5 mL) then suspended in THF (15 mL). Diphenylphosphine (0.606 g, 3.25 mmol) was added dropwise and the solution turned red, and clear, when no solid KH remained. Compound **4** (0.50 g, 1.08 mmol) in 2 mL THF was cannulated to the above red solution at -10 °C. Stirring was continued at -10 °C for 20 min, then at room temperature for an additional 40 min. The reaction was quenched by the addition of deoxygenated saturated NH_4Cl (5 mL). The mixture was stirred until the organic layer became clear (20 min). The organic layer was separated and the aqueous layer was washed with toluene (2 x 5 mL). The combined organic fractions were then dried over deoxygenated Na_2SO_4 , filtered, and concentrated under reduced pressure in a warm water bath. The resulting oily product could not be further purified. ^1H NMR (CDCl_3) δ 1.05 (dd, $J = 7.2, 16.5$ Hz, 3 H), 1.90 (m, 2 H), 2.29 (br, 1 H), 3.30 (m, 2 H), 3.72 (br, 1 H), 6.7-7.9 (m, 30 H); ^{31}P NMR (CDCl_3) δ -23.15, -20.61, 33.89.

$\text{CH}_3\text{CH}(\text{PPh}_2)\text{CH}(\text{CH}_2\text{PPh}_2)_2$ (6**)**

A 50 mL three neck flask was charged with a solution of crude tripod phosphine mono-oxide **5** (0.35 g, 0.55 mmol) in distilled *p*-xylene (20 mL). Distilled *n*-tributyl amine

(0.69 mL, 2.90 mmol) and trichlorosilane (0.37 mL, 3.67 mmol) were added. The reaction mixture was refluxing at 160 °C for 1 day. 0.55 mL trichlorosilane and 0.27 mL *n*-tributyl amine were added to the reaction mixture again. Two days later, 0.2 mL trichlorosilane was added to the mixture again. After another 4 days refluxing, the reaction mixture treated with 30 % deoxygenated aqueous NaOH (6 mL). The reaction mixture was stirred at 60 °C for 1.5 h until both layers became transparent. The layers were separated and the aqueous layer was back-extracted with toluene (2 x 5 mL). The combined organic layers were washed sequentially with 30 % deoxygenated aqueous NaOH (6 mL), deoxygenated distilled water (6 mL), 0.1 N HCl (8 mL), and deoxygenated distilled water (6 mL). The organic layer was dried over Na₂SO₄, filtered, and concentrated under reduced pressure to give oily product in 69.7% yield from ¹H NMR analysis. ¹H NMR (CDCl₃) δ 1.22 (dd, J = Hz, 3 H), 2.00(m, 3 H), 3.15 (br, 1 H), 3.30 (m, 1 H), 6.90-7.90 (m, 30 H); ³¹P NMR (CDCl₃) δ -23.81, -21.14, -9.67.

CH₃CH[P(O)Ph₂]CH[CH₂P(O)Ph₂]₂ (7)

The compound 5 (10.50 g, 16.41mmol) was dissolved in CH₂Cl₂ (100 mL, undistilled) and oxidized by adding a solution of 10 % H₂O₂ (60 mL). The reaction mixture was stirred for 10 min and then washed with a solution of saturated Na₂S₂O₃ (60 mL) until the excess H₂O₂ was neutralized (negative result with saturated solution of KI). The organic layer was dried over Na₂SO₄, filtered, and concentrated under reduced pressure affording tris(phosphine oxide) quantitatively. Crystallization from ether gave pure 7. ¹H NMR (CDCl₃) δ 1.20 (dd, J = 5.2, 12.4 Hz, 3 H), 2.19 (m, 1 H), 2.50 (m, 1 H), 2.81 (m, 1 H), 3.67 (br, 1 H), 3.89 (br, 1 H), 6.90-7.90 (m, 30 H); ¹³C NMR (CDCl₃) δ 4.98, 27.08, 29.40 (dd, J_{P-C} = 15.9, 16.8 Hz), 30.16 (dd, J_{P-C} = 13.0, 26.0 Hz), 31.57 (dd, J_{P-C} = 13.8, 70.1 Hz), 126.77, 126.87, 126.98, 127.07, 127.18, 128.59, 128.66, 128.90, 129.15, 129.32, 129.41, 129.61, 129.69, 130.04, 130.11, 130.33, 130.62, 131.16,

132.11, 132.54, 132.66, 133.53, 133.65; ^{31}P NMR (CDCl_3) δ 32.48, 33.09, 37.49. This tris(phosphine oxide) can also be obtained by oxidizing tripodal phosphine 6.

$\text{C}_6\text{H}_5\text{CH}=\text{C}(\text{COOMenth})_2$ (10, Menth = (1*R*, 2*S*, 5*R*)-(-)-menthol)

In air, dimethylmalonate (33.102 g, 87.1 mmol), dissolved in benzene (120 mL), was sequentially treated with acetic acid (1.0 mL, 17.4 mmol), piperidine (0.35 mL, 3.5 mmol), and benzaldehyde (10.0 mL, 95.8 mmol) in an azeotropic distillation apparatus. The mixture was refluxed at 120 °C for 1.5 h, then at 130 °C for an additional 24 h. Upon cooling to room temperature, benzene (100 mL) was added, and the resultant yellow-red solution was washed with 1 N HCl (2 x 100 mL), saturated NaHCO_3 (100 mL), and saturated NaCl (150 mL). The organic layer was dried over Na_2SO_4 , filtered, and concentrated under reduced pressure affording a yellow-white solid. The solid was recrystallized from methanol to afford 10 as pure white needle-shaped crystal in 89.5 % yield (36.53 g): m.p 103-104 °C; ^1H NMR (CDCl_3) δ 0.70-0.95 (m, 21 H), 1.05 (m, 3 H), 1.39 (m, 2 H), 1.50 (m, 2 H), 1.67 (br, 4 H), 1.81 (quint-d, $J = 6.9, 2.6$ Hz, 1 H), 1.92 (quint-d, $J = 6.9, 2.6$ Hz, 1 H), 2.07 (dbr, $J = 12.0$ Hz, 1 H), 2.13 (dbr, $J = 12.0$ Hz, 1 H), 4.85 (ddd, $J = 24.4, 10.9, 4.4$ Hz, 2 H), 7.25-7.40 (br, 3 H), 7.48 (m, 2 H), 7.68 (s, 1 H); ^{13}C NMR (CDCl_3) δ 15.87, 16.13, 20.81, 20.90, 22.00, 22.03, 22.91, 23.19, 25.35, 25.97, 31.32, 31.39, 34.07, 34.30, 40.22, 40.86, 46.70, 47.25, 75.39, 75.53, 127.31, 128.56, 129.40, 130.21, 133.02, 141.02, 163.59, 166.32. HRMS (EI). Calcd for $\text{C}_{30}\text{H}_{44}\text{O}_4$: 468.3240. Found: 468.3224. Anal. Calcd for $\text{C}_{30}\text{H}_{44}\text{O}_4$: C, 76.94; H, 9.47. Found: C, 76.79; H, 9.62.

$\text{C}_6\text{H}_5\text{CH}(\text{PPh}_2)\text{CH}(\text{COOMenth})_2$ ((*R*)-11 and (*S*)-11)

Method A: A solution of 10 (10 g, 21.3 mmol), *p*-toluenesulfonic acid monohydrate (0.1 g, 0.53 mmol), and diphenylphosphine (4.05 g, 21.76 mmol) in CH_2Cl_2

(100 mL) was stirred at room temperature for 72 h. The solution was stirred over NaHCO_3 (1 g) for 2 h, filtered, washed with toluene (3 x 10 mL), and concentrated under reduced pressure to afford a white solid in 100 % yield (13.97g). The solid was determined to be a mixture of both (*R*)-11 and (*S*)-11 in a 70 : 30 ratio. The solid was dissolved in toluene (20 mL) and methanol was added (300 mL) under reflux. White needle-like crystals of (*R*)-11 crystallized overnight and were isolated by filtration and washed with cold methanol (20 mL, 0 °C). The filtrate was concentrated under reduced pressure affording a white solid which was dissolved in boiling methanol (300 mL) and concentrated to 200 mL for crystallization. Solid cube-like crystals of (*S*)-11 were isolated by filtration and washed with cold methanol (20 mL, 0 °C). The filtrate was concentrated (~1/2 volume) and fractional crystallization afforded more (*R*)-11 and (*S*)-11. The combined portions of (*R*)-11 were recrystallized from toluene and methanol (1 : 20) affording white needle-like crystals of (*R*)-11 in 80.1 % yield (7.83 g): m.p 96 °C (oxidized); ^1H NMR (CDCl_3) δ 0.41 (d, $J = 6.9$ Hz, 3 H), 0.62 (q, 1 H), 0.70-0.80 (m, 10 H), 0.83-1.10 (m, 10 H), 1.18-1.35 (m, 2 H), 1.42-1.63 (m, 6 H), 1.69 (m, 2 H), 1.91 (m, 2 H), 3.94 (dd, $J_{\text{H-H}} = 12.1$ Hz, $J_{\text{P-H}} = 6.3$ Hz, 1 H), 4.39 (d, $J = 12.1$ Hz, 1 H), 4.45 (td, $J = 4.4$ Hz, 10.9 Hz, 1 H), 4.80 (td, $J = 4.4$ Hz, 10.9 Hz, 1 H), 6.68 (d, $J = 7.2$ Hz, 2 H), 6.91-7.03 (m, 3 H), 7.04-7.09 (m, 2 H), 7.13-7.18 (m, 2 H), 7.25-7.36 (m, 4 H), 7.55 (m, 2 H); ^{13}C NMR (CDCl_3) δ 15.69, 15.98, 20.84, 20.94, 21.98, 22.06, 22.93, 23.09, 25.50, 25.67, 31.20, 31.45, 34.12, 34.27, 40.05, 40.51, 44.93 (d, $J_{\text{P-C}} = 21.6$ Hz), 46.60, 47.06, 56.73 (d, $J_{\text{P-C}} = 31.8$ Hz), 75.38, 75.91, 126.20, 127.54, 127.82, 127.90, 128.21, 128.26, 128.36, 128.73, 129.42, 132.65, 132.82, 134.04 (d, $J_{\text{P-C}} = 14.8$ Hz), 135.52, 135.75, 135.88 (d, $J_{\text{P-C}} = 14.8$ Hz), 137.59, 166.93 (d, $J_{\text{P-C}} = 19.2$ Hz), 167.78.; ^{31}P NMR (CDCl_3) δ 4.36. HRMS (EI). Calcd for $\text{C}_{42}\text{H}_{55}\text{O}_4\text{P}$: 654.3838. Found: 654.3838. Anal. Calcd for $\text{C}_{42}\text{H}_{55}\text{O}_4\text{P}$: C, 77.03; H, 8.47. Found: C, 77.04; H, 8.73.

The combined portions of (*S*)-11 were recrystallized from pure methanol affording solid white cubes of (*S*)-11 in 63.9 % yield (2.68 g): m.p 95 °C (oxidized); ¹H NMR (CDCl₃) δ 0.45 (d, J = 5.9 Hz, 3 H), 0.65-1.00 (m, 20 H), 1.08 (m, 1 H), 1.25 (m, 2 H), 1.35 -1.65 (m, 6 H), 1.70 (m, 2 H), 2.08 (m, 2 H), 3.92(dd, J_{H-H} = 11.8 Hz, J_{P-H} = 8.7 Hz, 1 H), 4.39 (d, J = 11.8 Hz, 1 H), 4.51(td, J = 4.4, 10.9 Hz, 1 H), 4.80 (td, J = 4.4, 10.9 Hz, 1 H), 6.64 (d, J = 7.3 Hz, 2 H), 6.95-7.10 (m, 5 H), 7.15 (m, 2 H), 7.25-7.36 (m, 4 H), 7.55 (m, 2 H); ¹³C NMR (CDCl₃) δ 15.74, 16.49, 20.92, 21.88, 22.06, 22.92, 23.43, 25.33, 26.19, 31.20, 31.38, 34.10, 34.30, 40.26, 40.42, 45.13 (d, J_{P-C} = 23.3 Hz), 46.64, 46.97, 56.43 (d, J_{P-C} = 32.1 Hz), 75.29, 75.97, 126.23, 127.58, 127.81, 127.89, 128.12, 128.22, 128.27, 128.60, 128.62, 129.61, 132.38, 132.55, 133.64 (d, J_{P-C} = 16.3 Hz), 135.79, 136.02, 136.52(d, J_{P-C} = 15.4 Hz), 137.51, 167.21 (d, J_{P-C} = 19.5 Hz), 167.81; ³¹P NMR (CDCl₃) 7.92. HRMS (EI). Calcd for C₄₂H₅₅O₄P: 654.3838. Found: 54.3878. Anal. Calcd for C₄₂H₅₅O₄P: C, 77.09; H, 8.47. Found: C, 76.99; H, 8.47.

Method B: Potassium hydride (2.68 g, 22.43 mmol, 35% mineral oil dispersion) was charged into a 500mL flask and washed with THF (3 x 20 mL) then suspended in THF (150 mL). Diphenylphosphine (4.17 g, 22.39 mmol) was added dropwise over 15 min. when gas evolution stopped and the solution became red clear, this solution was immersed in a dry ice/acetone bath (-50 °C). A THF (50 mL) solution of 10 (10 g, 21.33 mmol) was added dropwise to the KPPH₂ solution over 40 min. Stirring was continued at this temperature for 30 min, then at room temperature for an additional 20 min. The reaction was quenched by the addition of deoxygenated saturated NH₄Cl (100 mL). The mixture was stirred until the organic layer became clear (20 min). The organic layer was separated and the aqueous layer was washed with toluene (3 x 50 mL). The combined organic layers were dried by MgSO₄. After the solvent was evaporated, the diastereomers were separated by fractional recrystallization as described above.

$C_6H_5CH[P(O)Ph_2]CH(CH_2OH)_2$ ((*R*)-12, (*S*)-12)

To a stirred mixture of $LiAlH_4$ (1.08 g, 28.46 mmol) and ether (100 mL) was added dropwise a solution of (*R*)-11 (6.5 g, 9.47 mmol) in ether (100 mL) at 0 °C over 10 min. The dropping funnel was rinsed with ether (50 mL), the reaction mixture was stirred for 20 min at 0 °C, and then for an hour at room temperature. The $LiAlH_4$ was neutralized by the dropwise addition of 1.1 mL of deoxygenated distilled water, 1.1 mL of deoxygenated 10% NaOH solution at 0 °C, and 3.3 mL of deoxygenated distilled water at room temperature. The mixture was stirred for 30 min, filtered, washed with CH_2Cl_2 (3 x 100 mL), and concentrated under reduced pressure yielding a white solid. The solid was recrystallized from toluene (100 mL) affording white crystals of the phosphine-diol. The phosphine-diol was dissolved in CH_2Cl_2 (400 mL, undistilled) and oxidized by adding a solution of 10 % H_2O_2 (35 mL). The reaction mixture was stirred for 5 min and then washed with a solution of saturated $Na_2S_2O_3$ (50 mL) until the excess H_2O_2 was neutralized (negative result with saturated solution of KI). The organic layer was dried over Na_2SO_4 , filtered, and concentrated under reduced pressure affording (*R*)-12 in 77.3 % yield (2.68 g), as a white powder. Further purification was unnecessary: 1H NMR ($CDCl_3$) δ 2.48 (m, 1 H), 3.25 (m, 2 H), 3.50 (dd, $J = 4.9, 10.7$ Hz, 1 H), 3.60 (dd, $J = 11.8, 8.1$ Hz, 1 H), 4.29 (dd, $J_{P-H} = 9.9$ Hz, $J_{H-H} = 3.5$ Hz, 1 H), 7.10-7.35 (m, 6 H), 7.40-7.60(m, 7 H), 7.92 (m, 2 H); ^{13}C NMR ($CDCl_3$) δ 44.06, 44.75, 60.52, 61.33 ($J_{P-C} = 11.8$ Hz), 127.35, 128.14, 128.25, 128.41, 128.82, 128.94, 130.92, 131.04, 131.23, 131.31, 131.36, 131.92, 132.11, 132.91 ($J_{P-C} = 3.1$ Hz); ^{31}P NMR ($CDCl_3$) δ 37.48. CIMS. (Carrier gas NH_3). Calcd for $C_{22}H_{23}O_3P$: 366.3972. Found: 367.4 (M+H), 368.3 (M+2H), 369.4 (M+3H). Anal. Calcd for $C_{22}H_{23}O_3P$: C, 72.12; H, 6.33. Found: C, 72.17; H, 6.11. (*S*)-12 was obtained by the same method.

$C_6H_5CH[P(O)Ph_2]CH(CH_2OMs)_2$ ((*R*)-13 and (*S*)-13)

To a solution of (*R*)-12 (2.50 g, 6.82 mmol) and dry triethylamine (2.85 mL, 20.46 mmol) in CH_2Cl_2 (250 mL) at -35 °C was added a solution of methanesulfonyl chloride (1.31 mL, 16.95 mmol) in dry CH_2Cl_2 (15 mL) over 10 min. The mixture was allowed to warm to room temperature over 1 h, and then stirred for an additional 45 min. In air, the reaction flask was placed in an ice bath and the solution was quenched by the addition of crushed ice (25 g), followed by cold water (25 g) with vigorous stirring. The ice bath was removed, and the solution stirred until the ice melted. The organic layer was separated, and the aqueous layer back-extracted with CH_2Cl_2 (50 mL). The combined organic layers were sequentially washed with cold water (2 x 60 mL), cold saturated $NaHCO_3$ (2 x 100 mL), and cold brine (2 x 60 mL). The organic layer was dried over Na_2SO_4 , filtered, and concentrated under reduced pressure to afford a light-yellow solid. The solid was recrystallized from methanol (10 mL) at -10 °C overnight affording white crystals of (*R*)-13 in 86.1 % yield (3.07 g): m.p 142-143 °C; 1H NMR ($CDCl_3$) δ 2.80 (s, 3 H), 2.80 (s, 3 H), 2.95 (m, 1 H), 3.87 (m, 2 H), 4.15 (d, $J = 6.1$ Hz, 2 H), 4.85 (dd, $J_{P-H} = 10.7$ Hz, $J_{H-H} = 2.9$ Hz, 1 H), 7.00-7.30 (m, 6 H), 7.30-7.60 (m, 7 H), 7.95 (m, 2 H); ^{13}C NMR ($CDCl_3$) δ 36.98, 37.07, 39.19, 43.38 (d, $J_{P-C} = 67.6$ Hz), 67.56 (m), 128.07, 128.15, 128.26, 128.96, 129.13, 129.25, 130.37, 130.43, 130.65, 130.74, 130.95, 131.04, 131.48, 131.95, 132.27, 132.35 (br); ^{31}P NMR ($CDCl_3$) δ 31.72. Anal. Calcd for $C_{24}H_{27}O_7PS_2$: C, 55.16; H, 5.21. Found: C, 54.93; H, 5.27. (*S*)-13 was obtained by the same method.

$C_6H_5CH[P(O)Ph_2]CH(CH_2PPh_2)_2$ ((*R*)-14, (*S*)-14)

Potassium hydride (3.25 g, 28.48 mmol, 35% mineral oil dispersion) was washed with THF (3 x 30 mL) then suspended in THF (100 mL). Diphenylphosphine (6.23 g, 33.49 mmol) was added dropwise turning the solution red, and clear, when no solid KH remained. (*R*)-13 (2.5 g, 4.78 mmol) was added at -10 °C in one portion as a powder.

Stirring was continued at $-10\text{ }^{\circ}\text{C}$ for 20 min, then at room temperature for an additional 40 min. The reaction was quenched by the addition of deoxygenated saturated NH_4Cl (10 mL). The mixture was stirred until the organic layer became clear (20 min) and a white precipitate remained. The organic layer was filtered from the white precipitate and the precipitate was washed with THF (2 x 20 mL). The combined organic fractions were then dried over deoxygenated MgSO_4 , filtered, and concentrated under reduced pressure in a warm water bath. The resulting oil was sonicated in the presence of hexanes (30 mL) leaving a white powder and clear solution. The mixture was filtered, the solid washed with hexanes (2 x 30 mL), and dried under reduced pressure. The solid was recrystallized from methanol affording white crystals of (*R*)-14 in 81.7 % yield (2.57 g): m.p $211\text{-}212\text{ }^{\circ}\text{C}$; $[\alpha]_{\text{D}} = -91.74^{\circ}$ (toluene, c 0.5047); $^1\text{H NMR}$ (CDCl_3) δ 1.70 (m, 2 H), 2.21 (br, 1 H), 3.10 (br, 1 H), 3.80 (m, 1 H), 4.68 (m, 1 H), 7.00-7.40 (m, 29 H), 7.56 (m, 4 H), 7.71 (br, 2 H); $^{13}\text{C NMR}$ (CDCl_3) δ 32.45 (m), 32.85 (m, two carbons overlapped), 46.95 (ddd, $J_{\text{P-C}} = 70.2, 10.9, 7.3\text{ Hz}$), 125.38, 127.29, 128.03, 128.14, 128.23, 128.31, 128.39, 128.47, 128.54, 128.88, 129.11, 130.76, 130.84, 130.97, 131.09, 131.17, 131.56, 131.99, 132.07, 132.13, 132.20, 132.31, 132.38, 132.69 (d, $J_{\text{P-C}} = 29.8\text{ Hz}$), 133.49, 133.68, 133.73 (d, $J_{\text{P-C}} = 10.7\text{ Hz}$), 134.24, 134.45, 136.28 (d, $J_{\text{P-C}} = 11.1\text{ Hz}$), 136.73 (d, $J_{\text{P-C}} = 13.6\text{ Hz}$), 138.71 (d, $J_{\text{P-C}} = 9.1\text{ Hz}$), 139.25 (d, $J_{\text{P-C}} = 10.3\text{ Hz}$); $^{31}\text{P NMR}$ (CDCl_3) δ 32.62, -20.99, -23.97. HRMS (EI). Calcd for $\text{C}_{46}\text{H}_{41}\text{OP}_3$: 702.2371. Found: 702.2372. Anal. Calcd for $\text{C}_{46}\text{H}_{41}\text{OP}_3$: C, 78.68; H, 5.88. Found: C, 78.37; H, 5.93. (*S*)-14 was obtained by the same method. $[\alpha]_{\text{D}} = +91.93^{\circ}$ (toluene, c 0.5058).

$\text{C}_6\text{H}_5\text{CH}(\text{PPh}_2)\text{CH}(\text{CH}_2\text{PPh}_2)_2$ ((*R*)-heliphos and (*S*)-heliphos)

A high pressure reactor was charged with a solution of (*R*)-14 (2.5 g, 3.56 mmol) in distilled *p*-xylene (20 mL). The reactor was placed in a $0\text{ }^{\circ}\text{C}$ ice-water bath. Distilled *n*-tributyl amine (5.04 mL, 21.2 mmol) and trichlorosilane (1.80 mL, 17.8 mmol) were

added, and the reactor was sealed. The reaction mixture was warmed to room temperature and then heated at 140 °C for 96 h. The reactor was cooled to room temperature, and the reaction mixture treated with 30 % deoxygenated aqueous NaOH (50 mL). The reaction mixture was stirred at 60 °C for 1.5 h until both layers became transparent. The layers were separated and the aqueous layer was back-extracted with toluene (2 x 25 mL). The combined organic layers were washed sequentially with 30 % deoxygenated aqueous NaOH (50 mL), deoxygenated distilled water (50 mL), 0.1 N HCl (75 mL), and deoxygenated distilled water (50 mL). The organic layer was dried over Na₂SO₄, filtered, and concentrated under reduced pressure. The remaining white solid was dried under reduced pressure for an additional 1 h then recrystallized from methanol affording white cube shaped crystals of (*R*)-heliphos in 82.0 % yield (2.00 g): m.p 140-141 °C ; [α]_D = -71.74° (toluene, *c* 1.0174); ¹H NMR (CDCl₃) δ 1.80 (br, 3 H), 2.99 (br, 1 H), 3.26 (br, 1 H), 4.59 (br, 1 H), 6.90- 7.60 (m, 35 H); ¹³C NMR (CDCl₃) δ 31.48 (m), 32.11 (m), 33.51 (m), 47.20 (dd, J_{P-C} = 8.5, 9.4 Hz), 126.64, 127.82, 127.89, 128.14, 128.14, 128.38, 128.44 (br), 128.83, 131.29, 131.38, 132.06, 132.15, 132.23, 132.33, 133.53, 133.72, 133.85, 134.05, 134.22, 136.44 (d, J_{P-C} = 14.3 Hz), 137.01(d, J_{P-C} = 4.9 Hz), 137.14 (d, J_{P-C} = 3.2 Hz), 137.39 (d, J_{P-C} = 14.1 Hz), 137.96 (d, J_{P-C} = 9.2 Hz), 139.54 (d, J_{P-C} = 10.9 Hz); ³¹P NMR (CDCl₃) δ -12.23, -21.72, -24.08. HRMS (EI). Calcd for C₄₆H₄₁P₃: 686.2421. Found: 686.2437. Anal. Calcd for C₄₆H₄₁P₃: C, 80.51; H, 6.02. Found: C, 80.68; H, 6.09. (*S*)-heliphos was obtained by the same method. [α]_D = +72.50° (toluene, *c* 0.5310).

[(heliphos)Rh(NBD)](ClO₄) (15)

A solution of [Rh(NBD)₂](ClO₄) (98.5 mg, 0.25 mmol) in CH₂Cl₂ (1.0 mL) at 0 °C was treated with a solution of (*R*)-heliphos (0.1752 g, 0.25 mmol) in CH₂Cl₂ (1.0 mL) added slowly with stirring. The yellow-red reaction mixture was stirred at room

temperature for 1 h. The solution was concentrated under reduced pressure and the resulting orange solid was washed with hexanes (3 x 5 mL). The solid was crystallized from methanol affording red-orange crystals of $[(R)\text{-heliphos}]\text{Rh}(\text{NBD})(\text{ClO}_4)$ in 88.2 % yield (216 mg): $[\alpha]_{\text{D}} = +127.18^\circ$ (toluene, c 0.5032); ^1H NMR (CD_2Cl_2) δ 1.41 (br, 2 H), 2.37 (dd, $J = 5.3, 16.2$ Hz, 1 H), 2.67 (dd, $J = 4.9, 15.2$ Hz, 1 H), 3.35 (m, 1 H), 3.55 (m, 5 H), 3.81 (d, $J = 9.0$ Hz, 1 H), 3.87 (br, 3 H), 6.27 (m, 2 H), 6.70 (m, 8 H), 7.00-7.35 (m, 15 H), 7.50 (br, 5 H), 7.12 (m, 3 H), 7.85 (m, 2 H); $^1\text{H}[^3\text{P}]$ NMR ($\text{CD}_2\text{Cl}_2:\text{CDCl}_3 = 1:1$) δ 1.44 (br, 2 H), 2.42 (d, $^2J_{\text{H-H}} = 16.2$ Hz, 1 H β *pro-S* (C13)), 2.68 (d, $^2J_{\text{H-H}} = 15.6$ Hz, 1 H β *pro-S* (C12)), 3.40 (dd, $^2J_{\text{H-H}} = 16.2$ Hz, $^3J_{\text{H-H}} = 7.0$ Hz, 1 H β *pro-R* (C13)), 3.49 (br, 2 H), 3.53 (br, 2 H), 3.63 (dd, $^2J_{\text{H-H}} = 15.6$ Hz, $^3J_{\text{H-H}} = 7.6$ Hz, 1 H β *pro-R* (C12)), 3.82 (s, 1 H β *pro-S* (C11)), 3.89 (br, 2 H), 3.98 (br, 1H), 6.28 (d, 2 H), 6.70 (m, 8 H), 7.00-7.35 (m, 15 H), 7.50 (br, 5 H), 7.12 (m, 3 H), 7.85 (d, 2 H); ^{13}C NMR (CD_2Cl_2) δ 25.26 (t, $J_{\text{P-C}} = 17.2$ Hz), 27.12 (dd, $J_{\text{P-C}} = 12.6, 20.4$ Hz), 37.83 (br), 44.27 (t, $J_{\text{P-C}} = 13.47$ Hz), 46.67, 46.91 (br), 47.42 (m), 61.82, 127.75, 127.86, 128.16, 128.61, 128.71, 129.05, 129.14, 129.53, 129.55, 129.64, 130.01, 130.10, 130.46, 130.70, 130.77, 130.88, 130.99, 131.48, 131.52, 131.59, 131.64, 132.25, 132.32, 132.43, 134.45 (d, $J_{\text{P-C}} = 5.4$ Hz), 134.78 (d, $J_{\text{P-C}} = 5.4$ Hz), 136.27, 136.59, 136.70, 136.83, 137.03 (d, $J_{\text{P-C}} = 10.8$ Hz), 139.95 (d, $J_{\text{P-C}} = 8.9$ Hz); ^{31}P NMR (CD_2Cl_2) δ -7.23 (ddd, $J_{\text{P-Rh}} = 111.6, J_{\text{P-P}} = 19.3, 35.9$ Hz), 0.765 (ddd, $J_{\text{P-Rh}} = 113.9, J_{\text{P-P}} = 19.3, 36.7$ Hz), 32.24 (pseudo-dt, $J_{\text{P-Rh}} = 116.7, J_{\text{P-P}} = 36.7, 35.9$ Hz). Anal. Calcd for $\text{C}_{53}\text{H}_{49}\text{P}_3\text{RhClO}_4$: C, 64.89; H, 5.04. Found: C, 64.89; H, 5.08. $[(S)\text{-heliphos}]\text{Rh}(\text{NBD})(\text{ClO}_4)$ was obtained by the same method. $[\alpha]_{\text{D}} = -128.64^\circ$ (toluene, c 0.4975).

Catalytic reactions

All glassware and syringes were treated with $\text{NH}_4\text{OH}/\text{EtOH}$, acetone, and oven-dried before use. The reactions were performed under anaerobic conditions (argon) in

rigorously dried solvents. All catalytic reactions were carried out using 1 mol % [((*R*)-heliphos)Rh(NBD)](ClO₄) as catalyst. ¹H NMR spectroscopy was used to calculate the chemical yield. The enantiomeric excess of each reaction was determined by analyzing the products as described below.

Hydrogenation

A typical procedure is given for the hydrogenation of methyl (*Z*)- α -acetamidocinnamate. A flask with one side-arm was oven-dried and flushed with Argon, then 5.0 mg (5.09 μ mol) [((*R*)-heliphos)Rh(NBD)](ClO₄), and 110.0 mg (0.50 mmol) methyl (*Z*)- α -acetamidocinnamate were charged into the flask. After 2 vacuum/argon cycles, the anhydrous degassed methanol (5 mL) was added to the flask. This flask was put into the high pressure reactor which had been flushed with Argon for 5 min. The high pressure reactor was sealed and purged with hydrogen for 2 min. The hydrogen pressure was raised to 4 atm and the reactor gas inlet was sealed. The reaction mixture was stirred at room temperature for 26 h. The solvent was removed at the end of the reaction by use of a rotary evaporator. The residue was dissolved in benzene and passed through a short SiO₂/Florisil column (benzene) to afford the pure methyl 2-acetamido-3-phenylpropanoate.

Hydroboration

A typical procedure is given for the hydroboration of styrene. [((*R*)-heliphos)Rh(NBD)](ClO₄) 5.00 mg (0.005 μ mol) was dissolved in 3 mL THF, and 52.7 mg (0.51 μ mol) styrene was added. Catecholborane (67.2 mg, 0.56 μ mol) was added at -30 °C, and the mixture was stirred at same temperature for 4 days and then quenched with 1 mL of methanol. To the mixture was added 1.2 mL of 3 M NaOH and 0.14 mL 30% H₂O₂, and it was stirred at room temperature for 3 h. Extraction with ether followed by

passing through a short SiO₂/Florisil column (hexane/ether = 1/1) gave quantitatively a mixture of 1-phenylethanol and 2-phenylethanol in 13 to 1 ratio from ¹H NMR analysis.

Hydrosilylation

A typical procedure is given for the hydrosilylation of acetophenone. A mixture of 63.0 mg (0.52 mmol) acetophenone and 5.0 mg (0.005 mmol) [(*R*)-heliphos)Rh(NBD)](ClO₄) was dissolved in 5 mL anhydrous, degassed THF. The diphenylsilane 198.6 mg (1.08 mmol) was added to the above mixture at -30 °C. The reaction was monitored by ¹H NMR spectroscopy. Upon completion the residue was dissolved in methanol (1 mL). To the solution was added sodium carbonate (0.2 mg) and the mixture was allowed to stir for 4 h. Following solvent removal, the alcohol was isolated by passing through a short column of Silica (SiO₂)/Florisil (hexane/ether = 1/1).

Enantiomeric excess determination

For methyl 2-acetamido-3-phenylpropanoate, ee was determined by mixing this product (50.0 mg) and tris[3-(trifluoromethyl-hydroxymethylene)-(+)-camphorate europium(III) (12.7 mg) in CDCl₃ and recording the ¹H NMR spectra. The ratio of the methoxy peaks at $\delta = 3.803$, $\delta = 3.697$ was used to determine the ee. The ratio of these peaks was 1 : 1 for racemic methyl 2-acetamido-3-phenylpropanoate.⁴⁶ For 2-phenylethanol, the ee was determined by ¹H NMR analysis of its Mosher's ester⁴² or by chiral capillary gas chromatography methods using a 30 m β -DEX 110 column purchased from Supelco Inc.

References

- (1) De Camp, W. H. *Chirality* 1989, 1, 2.
- (2) *Asymmetric Synthesis*; Morrison, J. D., Ed.; Academic Press: New York, 1983.
- (3) Borman, S. *Chem. Eng. News* 1990, 68 (28), 9.
- (4) Wong, C. H.; Whitesides, G. M. *Enzymes in Synthetic Organic Chemistry*; Pergamon: Oxford, 1994.
- (5) (a) Noyori, R. *Asymmetric Catalysis In Organic Synthesis*; Wiley Interscience, John Wiley and Sons: New York, 1994. (b) *Catalytic Asymmetric Synthesis*; Ojima, I., Ed.; VCH Publishers: New York, 1993.
- (6) Knowles, W. S. *Acc. Chem. Res.* 1983, 16, 106.
- (7) Inoue, S.; Takaya, H.; Tani, K.; Otauka, S.; Sato, T.; Noyori, R. *J. Am. Chem. Soc.* 1990, 112, 4897.
- (8) Aeatani, T. *Pure & Appl. Chem.* 1985, 57, 1837.
- (9) Gao, Y.; Hanson, R. M.; Klunder, J. M.; Ko, S. Y.; Masamune, H.; Sharpless, K. B. *J. Am. Chem. Soc.* 1987, 109, 5765.
- (10) (a) Whitesell, J. K. *Chem. Rev.* 1989, 89, 1581. (b) Brunner, H. *Angew. Chem. Int. Ed. Engl.* 1983, 22, 897.
- (11) Burk, M. J.; Harlow, R. L. *Angew. Chem. Int. Ed. Engl.* 1990, 29, 1462.
- (12) (a) Endo, I.; Horikoshi, S.; Utsumo, S. *J. Chem. Soc., Chem. Commun.* 1981, 296.
(b) Utsumo, S.; Miyamae, H.; Horikoshi, S.; Endo, I. *Inorg. Chem.* 1985, 24, 1348.
- (13) Canary, J. W.; Allen, C. S.; Castagnetto, J. M.; Wang, Y. *J. Am. Chem. Soc.* 1995, 117, 8484.
- (14) (a) Nugent, W. A. *J. Am. Chem. Soc.* 1992, 114, 2768. (b) Nugent, W. A.; RajanBabu, T. V.; Burk, M. J. *Science* 1993, 259, 479. (c) Nugent, W. A.; Harlow, R. L. *J. Am. Chem. Soc.* 1994, 116, 6142.
- (15) Brunner, H.; Rahman, A. F. M. M. *Chem. Ber.* 1984, 117, 710.

- (16) Adolfsson, H.; Wärmmark, K.; Moberg, C. *J. Chem. Soc., Chem. Commun.* 1992, 1054.
- (17) Trofimenko, S. *Chem. Rev.* 1993, 93, 943.
- (18) (a) Tokar, C. J.; Kettler, P. B.; Tolman, W. B. *Organometallics* 1992, 11, 2738. (b) LeCloux, D. D.; Tolman, W. B. *J. Am. Chem. Soc.* 1993, 115, 1153. (c) Cloux, D. D.; Tokar, C. J.; Osama, M.; Houser, R. P.; Keyes, M.; Tolman, W. B. *Organometallics* 1994, 13, 2856.
- (19) (a) Bianchini, C.; Meli, A.; Peruzzini, M.; Vizza, F.; Frediani, P.; Ramirez, J. A.; *Organometallics* 1990, 9, 226. (b) Bianchini, C.; Meli, A. *J. Chem. Soc., Dalton Trans.* 1996, 801. (c) Bianchini, C.; Herrera, V.; Jimenez, M. V.; Meli, A.; Sanchez-Delgado, R.; Vizza, F. *J. Am. Chem. Soc.* 1995, 117, 8567. (d) Ma, S.; Venanzi, L. M. *Tetrahedron Lett.* 1993, 34, 8071. (e) Sernau, V.; Huttner, G.; Fritz, M.; Zsolnai, L.; Walter, O. *J. Organomet. Chem.* 1993, 458, 63.
- (20) Burk, M. J.; Harlow, R. L. *Angew. Chem. Int. Ed. Engl.* 1990, 29, 146.
- (21) Ward, T. R.; Venanzi, L. M.; Albinati, A.; Lianza, F.; Gerfin, T.; Gramlich, V.; Tombo, G. M. R. *Helv. Chim. Acta* 1991, 74, 983.
- (22) Walter, O.; Klein, T.; Huttner, G.; Zsolnai, L. *J. Organomet. Chem.* 1993, 458, 63.
- (23) Heidel, H.; Huttner, G. *Z. Naturforsch.* 1993, 48 b, 1681.
- (24) Heidel, H.; Huttner, G.; Zsolnai, L. *Z. Naturforsch.* 1995, 50 b, 729.
- (25) (a) Schere, J.; Huttner, G.; Büchner, M. *Chem. Ber.* 1996, 129, 697. (b) Reinhard, G.; Soltek, R.; Huttner, G.; Barth, A.; Walter, O.; Zsolnai, L. *Chem. Ber.* 1996, 129, 97. (c) Seitz, T.; Muth, A.; Huttner, G. *Z. Naturforsch.* 1995, 50 b, 1045.
- (26) (a) Heidel, H.; Scherer, J.; Asam, A.; Huttner, G.; Walter, O.; Zsolnai, L. *Chem. Ber.* 1995, 128, 293. (b) Janssen, B. C.; Asam, A.; Huttner, G.; Sernau, V.; Zsolnai, L. *Chem. Ber.* 1994, 127, 501. (c) Seitz, Th.; Muth, A.; Huttner, G.; Klein, Th.; Walter, O.; Fritz, M.; Zsolnai, L. *J. Organomet. Chem.* 1994, 469, 155. (d) Muth, A.; Walter, O.; Huttner, G.; Asam, A.; Zsolnai, L.; Emmerich, C. *J. Organomet. Chem.*

- 1994, 468, 149. (e) Janssen, B. C.; Sernau, V.; Huttner, G.; Asam, A.; Walter, O.; Buchner, M.; Zsolnai, L. *Chem. Ber.* 1995, 128, 63., and references therein.
- (27) Beyreuther, S.; Hunger, J.; Huttner, G.; Mann, S.; Zsolnai, L. *Chem. Ber.* 1996, 129, 745.
- (28) (a) Brunner, H. In *Topics in Stereochemistry*; Eliel, E. L.; Wilen, S. H.; Ed., John Wiley & Sons: New York, 1988, 18, P129. (b) Pietrusiewicz, K. M.; Zablocka, M. *Chem. Rev.* 1994, 94, 1375. (c) Muci, A. R.; Campos, K. R.; Evans, D. A. *J. Am. Chem. Soc.* 1995, 117, 9075. (d) Schmid, R.; Broger, E. A.; Cereghetti, M.; Cramer, Y.; Foricher, J.; Lalonde, M.; Scalone, M.; Schoette, G.; Zutter, U. *Pure & Appl. Chem.* 1996, 68, 131., and references therein.
- (29) Takaya, H.; Akutagawa, S.; Noyori, R. *Org. Syntheses* 1988, 67, 20.
- (30) Mikhalev, O. V.; Malyshev, O. R.; Vinogradov, M. G.; Cheftsova-Bebutova, G. V.; Ignatenko, A. V. *Russ. Chem. Bull.* 1995, 44, 873.
- (31) Karplus, M. *J. Am. Chem. Soc.* 1963, 85, 2870.
- (32) Positions were calculated assuming idealized sp^3 geometries about the carbon atoms of the framework.
- (33) $[\text{Rh}(\text{triphos})(\text{NBD})](\text{ClO}_4)$ was prepared in situ in NMR tube by mixing equivalent amount of triphos and $[\text{Rh}(\text{NBD})_2](\text{ClO}_4)$ in CD_2Cl_2 .
- (34) Burgess, K.; Ohlmeyer, M. *Chem. Rev.* 1991, 91, 1179.
- (35) Brunner, H. *Angew. Chem. Int. Ed. Engl.* 1983, 22, 897.
- (36) Thaler, E. G.; Folting, K.; Caulton, K. G. *J. Am. Chem. Soc.* 1990, 112, 2664.
- (37) (a) Landis, C. R.; Halpern, J. *J. Am. Chem. Soc.* 1987, 109, 1746. (b) Halpern, J.; Ashby, M. T. *J. Am. Chem. Soc.* 1991, 113, 6429.
- (38) Wiles, J. A.; Lee, C. E.; McDonald, R.; Bergens, S. H. *Organometallics* 1996, 15, 3782.
- (39) Ashworth, T. V.; Chalmers, A. A.; Meintjies, E.; Oosthuizen, H. E.; Singleton, E. *Organometallics* 1984, 3, 1485.

- (40) Ashworth, T. V.; Chalmers, A. A.; Liles, D. C.; Meintjies, E.; Oosthuizen, H. E.; Singleton, E. *Organometallics* 1987, 6, 1543.
- (41) Carter, H. E.; Risser, W. C. *J. Biol. Chem.* 1941, 139, 255.
- (42) Dale, J. A.; Dull, D. L.; Mosher, H. S. *J. Org. Chem.* 1969, 34, 2543.
- (43) Rule, G. R.; Harrower, J. *J. Chem. Soc.* 1930, 2319.
- (44) Schenck, T. G.; Downes, J. M.; Milne, C. R. C.; Mackenzie, P. B.; Boucher, H.; Whelan, J.; Bosnich, B. *Inorg. Chem.* 1985, 24, 2334.
- (45) Powell, J.; Shaw, A. B. *J. Chem. Soc. (A)* 1968, 159.
- (46) Prepared by hydrogenation of (Z)-methyl- α -acetamidocinnamate by racemic [(heliphos)Rh(NBD)](ClO₄).